UNIVERSITY OF OKLAHOMA

GRADUATE COLLEGE

NEURAL SIGNATURES FOR PRECISION REHABILITATION IN STROKE AND AGING

A THESIS

SUBMITTED TO THE GRADUATE FACULTY

in partial fulfillment of the requirements for the

Degree of

MASTER OF SCIENCE

By

JORDAN WILLIAMSON

Norman, Oklahoma

2023

NEURAL SIGNATURES FOR PRECISION REHABILITATION IN STROKE AND AGING

A THESIS APPROVED FOR THE

STEPHENSON SCHOOL OF BIOMEDICAL ENGINEERING

BY THE COMMITTEE CONSISTING OF

Dr. Yuan Yang, Chair

Dr. Andriy Yabluchanskiy

Dr. Sarah Breen

Table of Contents

List of Tables and Figures

Abstract

The current growth of the population ages 65 and older is unprecedented. The number of these individuals is projected to nearly double by 2060 with the age group's share of total population rising from 16 to 23 percent. With the growing number of older adults, there is also an increase in the demands of the public health system. Chronic noncommunicable diseases associated with age are on the rise, such as dementia, cardiovascular diseases including stroke, diabetes, and cancer. Therefore, the study of these conditions is critically important, not only because these diseases cause a significant loss of function, but also to reduce the burden on the caregiving and healthcare systems. The aim of this thesis is to explore neural signatures of stroke and aging related conditions for the development of precision interventions and treatments. The research on stroke includes early data of a pilot clinical trial on the use of a novel precision rehabilitation technique for improving upper extremity motor function post stroke, as well as research on cortical reorganization in the somatosensory area post stroke. The work on aging investigates sex-specific functional connectivity biomarkers in both the prodromal stage of Alzheimer's Disease (AD), i.e., mild cognitive impairment, and AD. Beyond this thesis, the relationship between stroke and AD will be explored as our future work.

Chapter 1: Introduction

In 2020, 55.7 million adults were 65 or older in the United States, representing 1 in every 6 Americans. The current growth of this population is unprecedented, as number of individuals ages 65 and older is projected to nearly double by 2060 with the age group's share of total population rising from 16 to 23 percent [1, 2]. This shift in the distribution towards older ages is driven by a variety of factors, including declines in fertility and birthrate, improvements in longevity, and the aging of the large Baby Boomer generation born between 1946 and 1964 [2, 3].

With the growing number of older adults, there is an increase in the demands of the public health system. In particular, chronic noncommunicable diseases associated with age are on the rise, such as dementias, cardiovascular diseases including stroke, diabetes, and cancer [3]. It is projected that by 2030, 60% of individuals 65 and older will be managing more than one chronic condition. These conditions are the national leading drivers of disability, diminishment of quality of life, death, and health and long-term care costs [4]. In fact, 90 percent of the national 4.1 trillion in annual health care expenditures are for people with chronic and mental health conditions [5]. Therefore, the study of these conditions is critically important, not only because these diseases cause a significant loss of function, but also to reduce the burden on the caregiving and healthcare systems.

This work focuses on targeted precision care for individuals who are impaired post stroke and individuals with Alzheimer's Disease (AD). Precision medicine seeks to maximize the quality of care through a shift from a one-size-fits-all to an individualized approach. It recognizes the heterogeneity of patient characteristics and aims to deliver optimally targeted and timed interventions tailored to individual's molecular drivers of disease [6]. Research in precision healthcare includes a wide variety of fields including drug discovery, biomarker identification,

estimation and inference for casual treatment effects, and modeling health communication [7]. Neurological diseases are particularly well suited for precision medicine due to the ability to assess targeted diagnostic biomarkers, the rapidly expanding genetic knowledge base, and the development of targeted pathways [8]. Therefore, the aim of this thesis is to explore neural signatures of stroke and AD for the development of precision interventions and treatments. The research on stroke includes early data of a pilot clinical trial on the use of a novel precision rehabilitation technique for improving upper extremity motor function post stroke, as well as research on cortical reorganization in the somatosensory area post stroke. The work on Alzheimer's investigates sex-specific functional connectivity biomarkers in both the prodromal stage of AD, i.e., mild cognitive impairment, and AD. Beyond this thesis, the relationship between stroke and AD will be explored as our future work.

Chapter 2: Stroke and Rehabilitation

2.1 Background

Stroke occurs when the blood supply to the brain is reduced or blocked completely, which prevents brain tissue from getting oxygen and nutrients and can increase pressure in the surrounding tissue causing swelling. Without oxygen and nutrients, brain cells begin to die within minutes [9]. Strokes are classified into two main categories, ischemic and hemorrhagic strokes. An ischemic stroke occurs when a blood vessel becomes blocked and impairs blood flow to part of the brain. This can be a thrombotic ischemic stroke when the blood clot develops in the blood vessels inside the brain, or an embolic ischemic stroke when a blood clot or plaque debris develops in another part of the body and travels to the brain [10]. A hemorrhagic stroke occurs when a blood vessel that supplies blood to the brain ruptures and bleeds. This can be intracerebral hemorrhage which is bleeding from the blood vessels within the brain, or a subarachnoid hemorrhage which is bleeding space between the brain and membranes that cover the brain [10]. Stroke remain a compelling public health issue as more than 795,000 people United States experience a stroke each year. Stroke is the fifth leading cause of death and the leading cause of serious long-term disability [11]. Stroke recovery is heterogeneous, since the long-term effect of a stroke is determined by the site and size of the initial lesion [12]. Specifically, a stroke that occurs in the motor and somatosensory cortices will cause focal damage to the cortices and to their descending pathways [13]. This causes a variety of physical effects, including hemiparesis, loss of sensation in the extremities, spasticity, and loss of fine motor skills. The ability of the human brain to recover from these post stroke motor and sensory impairments is mainly done through neuroplasticity [14]. Neuroplasticity is defined as a change or rewiring in the neural network. For a neural modulatory rehabilitation intervention to

successfully cause plasticity it must be task specific, and goal directed. To do this, how the brain originally reorganizes post stroke must be considered [15]. Therefore, the first study on this work on post stroke rehabilitation is focused on subject specific neural modulation to facilitate recovery of motor function. The second study investigates somatosensory system reorganization and its relation to movement impairments.

2.2 Stroke Study 1: Subject specific neural modulation to facilitate recovery of motor function.

Objectives

Upper-extremity motor impairments include muscle weakness, abnormal muscle synergies, and spasticity [16]. Both animal and human studies of stroke survivors suggest and support the role of cortico-reticulospinal tract (CRST) hyperexcitability in the contralesional hemisphere in more severe impairments post-stroke [17, 18], in particular, the expression of the prevalent abnormal muscle synergies in the paretic upper limb [19, 20]. CRST hyperexcitability in the contralesional hemisphere emerges as a consequence resulted from damage to the ipsilesional motor cortex or its descending pathway, i.e., the corticospinal tract (CST) [18]. The medial CRST primarily originates from the dorsal premotor cortex (PMd) and travels through the pontine reticular formation [21]. Previous studies applying transcranial magnetic stimulation (TMS) to patients after stroke demonstrated that the medial CRST is responsive to the excitatory ipsilateral input from the PMd in the contralesional hemisphere [22, 23]. This finding makes the contralesional PMd (cPMd) a potential target for combating moderate-to-severe movement impairment. Thus, our key hypotheses are that: 1) facilitating the ipsilesional primary motor cortex (iM1) improves the excitability of the damaged CST, thus, reducing the CRST hyperexcitability

and motor impairments, 2) inhibiting the contralesional dorsal premotor cortex (cPMd) directly reduces the CRST hyperexcitability and thus, may also improve motor behaviors.

Recent studies demonstrated that *transcranial direct current stimulation* (tDCS) could be a safe and quick approach to modulate cortical excitability [24]. However, the effect of conventional tDCS is limited as it uses large size "sponge" electrodes, making it difficult to target a specific region of interest in the brain for testing the hypothesis. To address the limitation of conventional tDCS that non-specifically activates many brain areas, we propose to use a targeted *high-definition tDCS (HD-tDCS)* with a few small electrodes and, navigated by subject-specific MR-based computer simulation [25] and verified by TMS localization technique, to specifically modulate the targeted cortical regions. The overall objective of this proof-of-concept study is to explore the potential of targeted HD-tDCS to modulate the excitability of specific cortical motor regions and their underlying motor pathways to diminishing post-stroke upper limb impairments.

Methods

Ten ischemic stroke (at least 3 months after a stroke) participants (two females) consented and screened for this study with their Fugl-Meyer upper extremity (FMUE) scores [26]. The study is approved by the internal review board (IRB) of the University of Oklahoma Health Sciences Center (IRB # 14011). The demographics of stroke participants are provided in **Table 2.2.1**, including participants Fügl-Meyer Upper Extremity score (FM-UE).

Table 2.2.1 Stroke Participants Demographics

Subject ID	Lesion Side	Paretic Side	Age	Sex	Hispanic/Latino	Race	Time post stroke	FM-UE (Total:66)
S1	L	R	64	M	No	Asian	33 months	8
S2*	R	L	72	M	No	White	17 months	14
S3*	L	R	81	F	No	White	14 months	10
S4	Both	L	55	M	No	White	6 months	46
S5*	L	R	44	M	No	White	3 months	26

S6	R	L	62	M	No	White	30 months	48
S7	L	R	43	M	No	White	87 months	53
S8	R	L	59	M	Yes	White	33 months	46
S9*	R	L	65	M	No	White	14 months	16
S10*	L	R	73	F	No	White	92 months	23

*Participants who attended HD-tDCS sessions

The transcranial magnetic stimulation (TMS)-induced motor-evoked potentials (MEP) were assessed determine the use of the ipsilesional corticospinal tract and the contralesional cortico-reticulospinal tract [22, 23], with the MEP latency/status as the outcome measure [22, 27]. The paired-pulse TMS (Magstim® BiStim^2, The Magstim Company Ltd., Spring Gardens, Whitland, UK) was applied at the respective hotspots for the elbow flexor muscle at the paretic arm, i.e., Biceps Brachii, over the ipsilesional primary motor cortex (iM1, from which the corticospinal tract originates) and contralesional dorsal premotor cortex (cPMd, from which the cortico-reticulospinal tract originates) with reference to the paretic arm, using a figure-eight coil [22]. We used the paired-pulse TMS with a conditioning pulse (65% stimulator maximum intensity) followed by a testing pulse (85% stimulator maximum intensity), to avoid the need to pre-activate the muscle (which could cause the bias of background EMG) [28], with paired-pulse intervals of 25ms [22]. The center of the coil was positioned tangentially to the skull with the handle at 45° from the parasagittal plane: posterior-anterior orientation for iM1 and anterior-posterior orientation for cPMd (Fig. 1) [29, 30]. The M1 hotspot is defined as the grid-point that results in the largest response in the target muscle, and was found for the ipsilesional (iM1) and the contralesional (cM1) hemisphere through stimulation of a 5 x 5 grid of 1 cm spaced sites on the scalp over motor areas of each hemisphere (centered at C3/4 of 10-20 EEG system) [27]. The "hot-spot" of cPMd was identified using a reference point of 1 cm medial and 2.5 cm anterior of the M1 "hot-spot" at the contralesional hemisphere [29, 31]. We determined MEP status using criteria previously reported [32]: the patient was considered MEP+ if MEPs of any amplitude are

observed at a consistent latency on at least 5 out 10 trials; otherwise, MEP– . After determining the status of MEP, at least eight more pulses (inter-stimulus interval: 2-3s) were applied to the identified hotspot to get a robust estimate of the latency of the MEP. We calculated average latency across all positive trials to determine the latency of MEP.

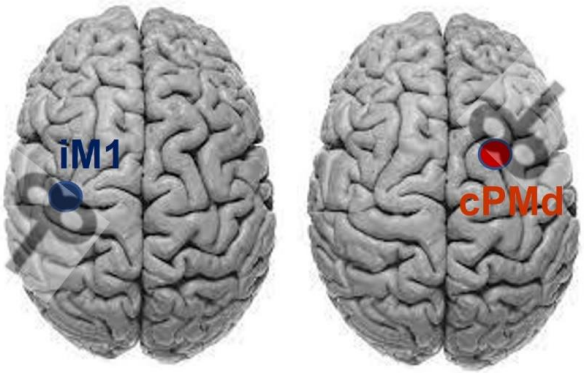

Figure 2.2.1 Coil orientation for stimulating ipsilesional primary motor cortex (iM1) and contralesional dorsal premotor area (cPMd). Assuming the lesion on the left side.

Five of the participants (S2, S3, S5, S9 and S10) who are more severely impaired (FMUE: 10-31) with detectable ipsilateral MEP from the contralesional dorsal premotor cortex (cPMd) and met the inclusion/exclusion criteria of a registered pilot clinical trial (ClinicalTrials.gov Identifier: NCT05174949).

Inclusion Criteria:

- Ischemic unilateral, subcortical stroke lesion (confirmed by the most recent clinical or radiological reports) at least 3 months prior to participation in this project.
- Paresis confined to one side, with moderate to severe motor impairment of the upper limb (Fugl-Meyer upper extremity scores between 10-40 out of 66 at the first visit of this study).
- Capacity to provide informed consent.

Exclusion Criteria:

- Muscle tone abnormalities and motor or sensory impairment in the unimpaired limb.
- Severe wasting (Fugl-Meyer upper extremity scores below 10) or contracture or significant sensory deficits in the paretic upper limb.

- Severe cognitive or affective dysfunction that prevents normal communication and understanding of consent or instruction.
- Severe concurrent medical problems (e.g. cardiorespiratory impairment).
- Using a pacemaker.
- Metal implants in the head.
- Known adverse reaction to TMS and tDCS.
- Pregnant.

These five participants continued to participate in this randomized, double-blinded (Participant, Outcomes Assessor) cross-over pilot trial with three visits: 1) anodal high-definition transcranial direct stimulation (HD-tDCS) over the ipsilesional primary motor cortex (iM1), 2) cathodal HD-tDCS over cPMd, 3) sham stimulation, with a two-week washout period in-between.

The proposed HD-tDCS method uses five small electrodes with the main stimulation electrode in the center, and four surrounding co-centric electrodes with opposite polarity. The HD-tDCS electrodes were mounted onto a standard 10-20 EEG cap. The stimulation dosage was set as 2 mA, for 20 min, the optimal safe dosage to influence neuroplasticity according to the safety guidelines of HD-tDCS [33, 34]. The stimulation location was identified using **subject-specific** 1.5T MR images and verified by the TMS-induced MEP as explained above, with the center electrode on the TMS "hot-spot" and 40-45 mm (depending on the size of the head) distance between the center and surrounding electrodes [22, 27]. This is the optimal distance based on our previous simulation study [25]. Electrical fields in the brain were estimated using the Realistic Volumetric Approach to Simulate Transcranial Electric Stimulation (ROAST) toolbox to confirm that the targeted brain area was stimulated (as illustrated in **Figure 2.2.2**) [35]. The effect of HD-tDCS is determined by the change of MEP latencies and amplitude (primary outcome measures), and Improvement Index (secondary outcome measure) that is derived from the FM-UE:

Improvement Index = (Post Score – Pre Score)/ Pre Score. Statistical analyses were performed by our biostatistician Dr. Shirley James, using commercial software Statistical Analysis Systems (9.4, SAS, Carey, NC, USA). After checking for and finding no evidence of a non-normal outcome measure distribution, we analyzed the data using generalized estimating equation (GEE) using PROC GENMOD. The fixed factors are group (anodal, cathodal, sham), time (pre and post intervention), with their interaction, and the random factor is subject ID. This technique uses correlated linear models for each outcome variable.

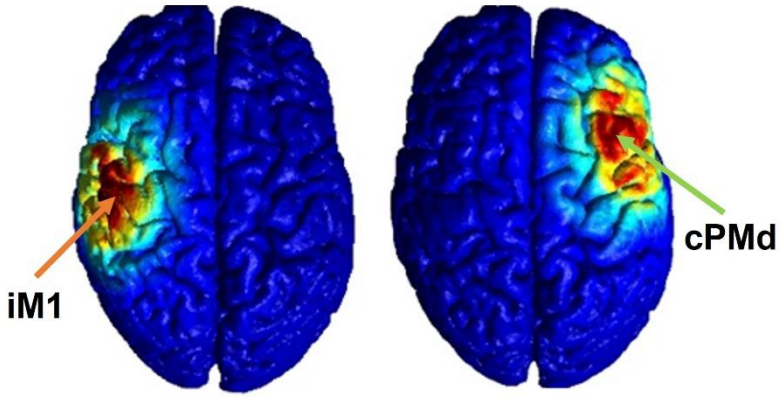

Figure 2.2.2 Electrical field estimation for iM1 (left) and cPMd (right) HD-tDCS.

Results

The iM1-induced contralateral MEP (iM1 MEP) was detected in all ten participants. An example MEP response is provided in **Figure 2.2.3**. The latency of the iM1 MEP was negatively correlated with FM-UE score (correlation coefficient r = - 0.96, p < 0.001, see **Figure 2.2.4**). Moreover, the latency of the iM1 MEP was predictive of FM-UE scores (determination of correlation: R^2 = 0.9197). The amplitude of the iM1 MEP was positively correlated with FM-UE score (correlation coefficient r = 0.92, p <0.001, see **Figure 2.2.5**). The amplitude of iM1 MEP was also predictive of FM-UE scores (determination of correlation: R^2 = 0.8464).

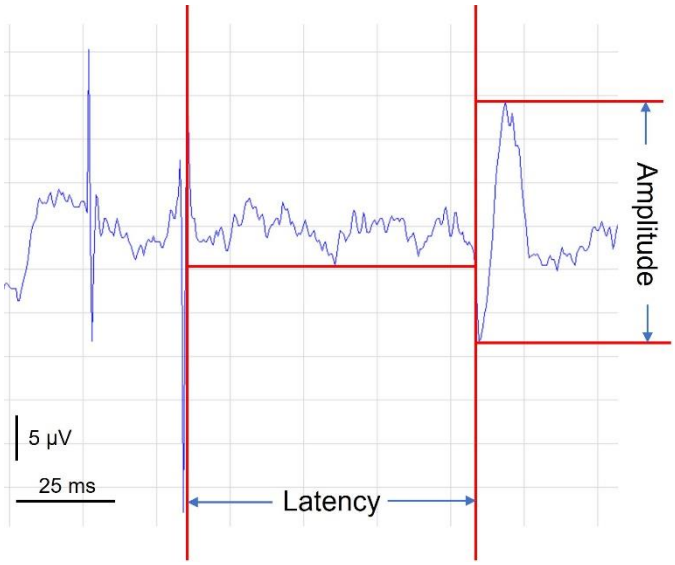

Figure 2.2.3 Example of MEP response and interpretation

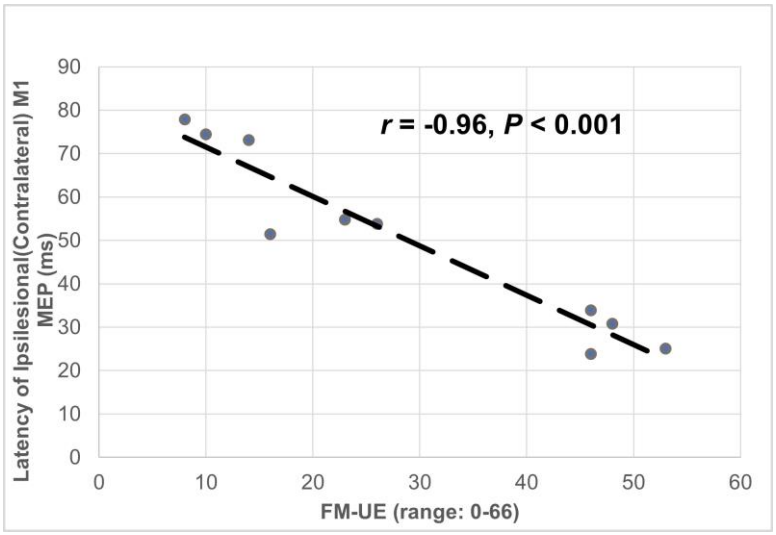

Figure 2.2.4 Correlation between the latency of ipsilesional (contralateral) M1 MEP and FMUE

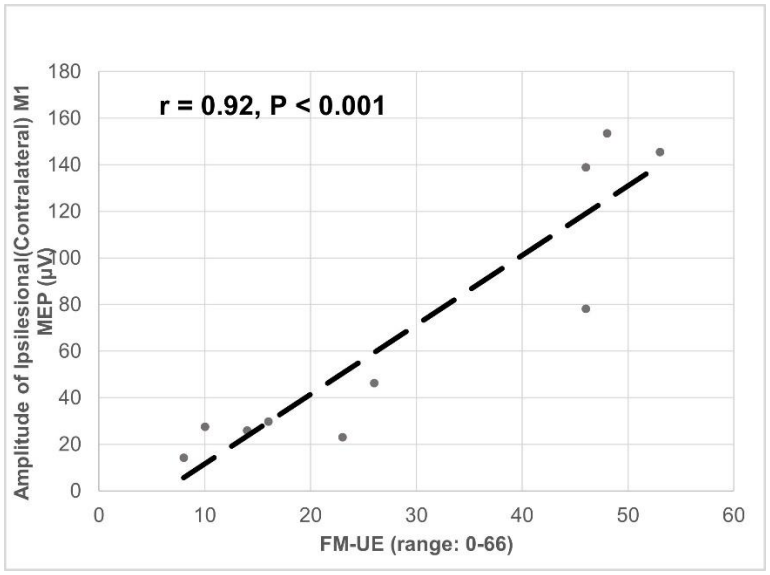

Figure 2.2.5 Correlation between the amplitude of ipsilesional (contralateral) M1 MEP and FMUE

For those moderate-to-severe subjects (S2, S3, S5, S9 and S10) who attended the HD-tDCS sessions, GEE analysis of the iM1 MEP latency using SAS 9.4 revealed when compared to the sham group, the anode group (group*time) changed significantly differently after intervention with a beta estimate of -30.5, z=-13.37, and p<0.0001. The cathode group (group*time) also changed significantly differently over time compared to the sham with beta estimate of -25.7, z=-10.97, and p<0.0001 (see **Figure 2.2.6).** There was no significant statistical difference between either anodal or cathodal stimulation compared to sham on MEP amplitude.

Only moderate-to-severe participants had a detectible ipsilateral MEP response when stimulating the contralesional dPM (i.e., cPMd MEP). The cPMd MEP either disappeared or was delayed after active (anodal/cathodal) HD-tDCS but not after the sham stimulation (**Table 2.2.2**).

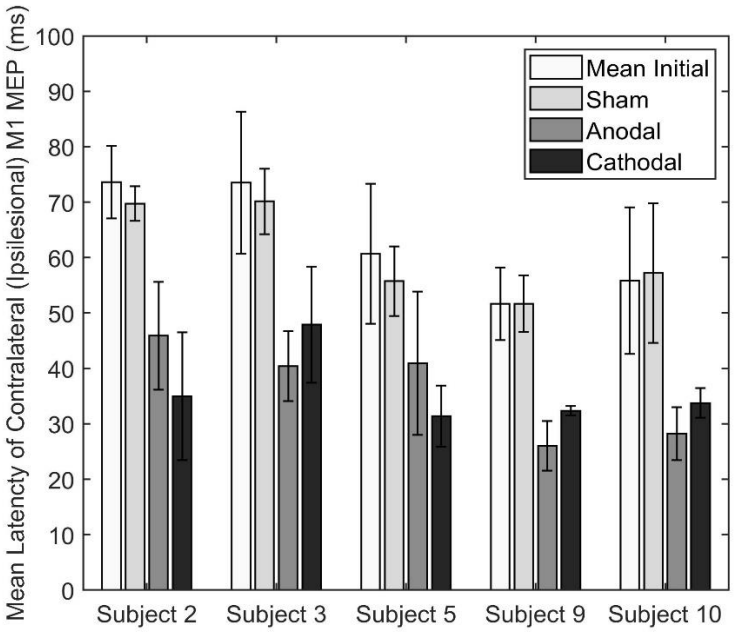

Figure 2.2.6 iM1 MEP latency pre and post HD-tDCS stimulation (sham, anodal, and cathodal)

Table 2.2.2 The mean latency of ipsilateral (contralesional) cPMd MEP

Subject ID	Initial	Sham	Anodal	Cathodal
S2	58.47 ms	63.65 ms	(-)	(-)
S3	89.96 ms	90.88 ms	107.05 ms	106.73 ms
S5	91.03 ms	88.60 ms	(-)	103.53 ms
S9	86.34 ms	92.70 ms	105.48 ms	(-)
S10	82.31 ms	76.60 ms	110.76 ms	(-)

The change of FM-UE over time post HD-tDCS using GEE analysis in SAS 9.4 revealed when compared to the sham group, the anode group (group*time) changed significantly differently over time with a beta estimate of 7.8 with z=2.4E15 and p<0.0001. The cathode group (group*time) also changed significantly differently over time compared to the sham with beta estimate of 5.6, z=9.86E14, and p<0.0001.

The individual results show that the anodal HD-tDCS improved FM-UE score in all five subjects, while the cathodal HD-tDCS demonstrated its effort in four subjects but not the one with a relatively higher FM-UE score (FM-UE = 26, see **Figure 2.2.7**). The anodal HD-tDCS demonstrated the largest FM-UE score improvement in the subject (S5) who has the highest FM-UE score (FM-UE = 26) while the cathodal HD-tDCS showed the largest improvement in the subject (S3) who has the lowest FM-UE score (FM-UE = 10).

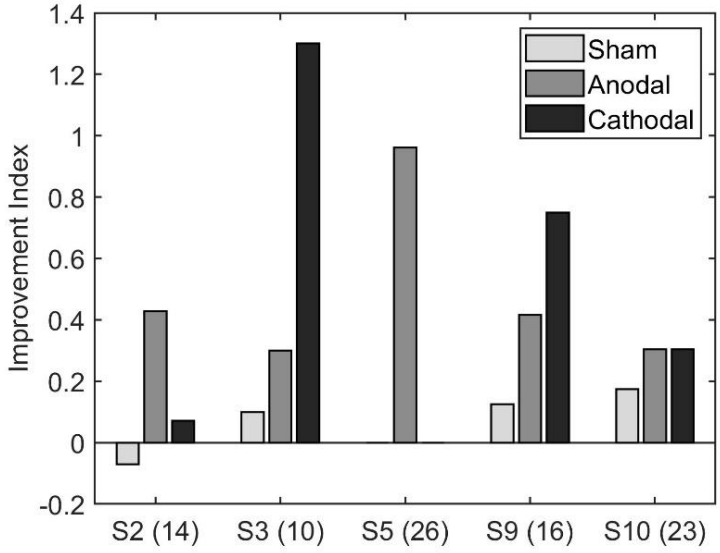

Figure 2.2.7 Improvement Index of sham, anodal, and cathodal stimulation. Values in parathesis indicate the initial FMUE score of subjects.

Discussion

This study supports the use of both targeted anodal and cathodal HD-tDCS as a method for rehabilitation post-stroke. The relationship between the FM-UE motor score and the latency and amplitude of contralateral (ipsilesional) iM1 TMS-induced MEP is consistent with prior studies on MEPs and clinical assessments post-stroke [36-38]. This finding confirmed that change in latency and amplitude have the potential to be good predictors of functional change of motor

descending pathways post HD-tDCS stimulation and the selection of them as primary outcome measures of this study.

We observed that facilitating iM1 using anodal HD-tDCS decreased the latency of iM1 TMS-induced MEP in all five subjects. The change in latency was significantly different between anodal and sham stimulation. The anodal stimulation was also associated with increased FM-UE scores in all five subjects, with the largest improvement in the subject with the highest initial score. The minimally clinically important difference for the FM-UE ranges from 4.25-7.25 points [39]. A difference greater than 6.0 was observed in four out five subjects, with S10 having a difference of 4.0 points. The increase in FM-UE scores reflects an improvement in overall arm function of the upper extremity post anodal stimulation. This improvement is consistent with prior studies on anodal HD-tDCS at iM1 post stroke [40, 41]. However, this study further demonstrates that anodal stimulation may specifically improve the excitability of the damaged CST and improve motor impairments. More importantly, the facilitation of the CST may also reduce hyperexcitability in the CRST, as post anodal stimulation the latency of cPMd TMS-induced MEP was either delayed, or not detected. This is likely because the increased cortical excitability of iM1 may enhance the super bulbar inhibition to the reticulospinal tract via the cortico-reticular pathways [21]. While the amplitude was correlated to the baseline of impairment with the FMUE score, there was not a significant change in amplitude pre and post HD-tDCS stimulation. The results of the change in MEP amplitude post tDCS stimulation are highly variable in the literature [38, 42, 43]. In fact, recent reviews and studies have shown that MEP amplitude is not a sufficiently robust measure of tDCS at low intensities [44, 45]. The results of this pilot study provide some preliminary evidence that MEP latency may be a better predictor of the neurophysiology effect of tDCS.

Furthermore, inhibiting the cPMd decreased the latency of iM1 TMS-induced MEP in all five subjects and the change in latency was significantly different between cathodal and sham stimulation. The cathodal stimulation improved the FM-UE score in 4 out and 5 subjects, with no change in the subject with the highest initial score and the largest increase in the subject with the lowest initial score. These results may indicate that cathodal stimulation has a greater effect in more impaired individuals with higher levels of spasticity due to hyperexcitability of CRST. This indicates that inhibiting the cPMd leads to a reduced recruitment of CRST, which is known as the key drive of post-stroke spasticity [18]. Based on previous research, this result may be related to decreased input to descending monoaminergic pathways at the Ponto-medullary reticular formation that reduce the hyperactivity of alpha motoneuron pool at spinal cord [46].

This finding may play a key role in developing an alternative intervention for severely impaired stroke survivors exhibiting increased levels of spasticity. Despite the development of a variety of interventions for movement recovery, rehabilitation treatments are minimally effective for more impaired individuals, making this finding especially clinically relevant. Currently, botulinum toxin has been increasingly used to treat upper limb spasticity in chronic stroke. Botulinum toxin is injected locally into the muscle and causes temporary paresis by blocking cholinergic transmission [47]. While this can reduce muscle tone, there is currently not a significant difference in improved arm function and no guidelines for dosage [48-50].

Overall, this study improves our understanding of neural circuitry and plasticity post stroke by confirming neural targets (iM1 and cPMd) for motor descending pathways. It also shows the benefit of subject specific precise neuro-navigation to guide the stimulation. The promising result for more impaired individuals is highly significant as it may provide an alternative intervention

option to those experiencing high spasticity and abnormal muscle synergy patterns with limited options for improving their upper limb function.

Limitations and Future Work is related to the limited sample size in this pilot trial, the sole use of stroke subjects at least 3 months post stroke, and the lack behavioral tasks during HD-tDCS stimulation. Within this pilot study we included only stroke participants at least 3 months post stroke because in the acute phase, stroke survivors typically experience some degree of spontaneous motor and sensory recovery [51] and currently attend a physical therapy rehabilitation program [52]. After the first 3 months in stroke recovery timeline, spontaneous motor and sensory improvement reaches a plateau [53]. These covariates make it difficult to determine the sole impact of HD-tDCS. Therefore, this study used chronic stroke participants in a cross-over study designed to reduce type I error. However, this protocol of HD-tDCS may be a useful addition to the acute phase. Hence, future work would be a larger clinical trial utilizing both acute and sub-acute groups. Although, other research has linked a concurrent behavioral task, such a mirror therapy, with tDCS has shown a boost in post-stimulation performance [54, 55]. This study's aim was to exclusively examine the feasibility of HD-tDCS on modulating the function of motor descending pathways. A future study could include the addition of a behavioral task to further explore its potential to improve current intervention practice of stroke rehabilitation.

2.3 Stroke Study 2: Determine cortical sensory impairment and reorganization post stroke

Objectives

The control of movement requires somatosensory feedback. However, how the somatosensory system adapts to the change in the use of motor pathways and the role of adaptive sensory feedback to the abnormal movement control of the paretic arm remains largely unknown. The ascending sensory pathways that convey somatosensation from the paretic arm project

contralaterally to the primary sensory cortex in the lesioned hemisphere. It is unknown, however, whether a similar hemispheric shift in cortical somatosensory processing after a stroke occurs may be related to the maladaptive use of contralesional cortico-reticulospinal pathways and motor impairment [11]. The answer to this question is important since it may permit a potential assessment of motor deficits from a sensory perspective, which could be clinically significant in more severely impaired individuals who can barely perform any functional movement tasks, as well as in individuals in the acute/subacute phases of recovery from a stroke whose movement ability is still limited or absent. This also prevents "over-exerting" a more impaired individual or an acute individual while performing motor assessments or strenuous non-targeted rehabilitative interventions thus encouraging the maladaptive use of reticulospinal pathways resulting in the emergence and expression of the flexion synergy and spasticity after a stroke [56].

To explore this question, this proof-of-concept study assessed the cortical somatosensory processing in chronic stroke patients and compared it with that in age-matched control subjects. The electroencephalogram (EEG) was recorded when the participants are receiving electrical tactical index finger stimulation to investigate cortical somatosensory processing based on somatosensory evoked potentials (SEP) and source localization. Electrical stimulation of the index finger was selected because we aimed to target exclusively Aβ sensory fibers. Aβ fibers provide pure tactile sensory information, compared to the commonly stimulated, more proximal portion of the median nerve at the palm or forearm that provides both sensory (tactile and muscle afferents) and motor activity to the forearm, wrist, and hand muscles [57, 58]. Cutaneous Aβ fibers, even though thicker than Aδ and C fibers, are thinner than group I and II muscle afferents and stimulated more distally at the index finger, thus resulting in a longer time delay to the primary motor cortex of greater than 20ms [59]. Therefore, based on the literature, components P50 and N100 of the

SEP were selected as time points of analysis since they are the earliest SEP components where little integration from other cortical areas took place, yet long enough to get a SEP response not contaminated by the stimulation artifact [60-63].

Methods

Nine individuals' post-stroke (three females) and eight age-matched healthy controls (four females) participated in this study. The study is approved by the internal review board (IRB) of the University of Oklahoma Health Sciences Center (IRB # 12550). The demographics of stroke participants are provided in **Table 2.3.1**, including participants' Fügl-Meyer Upper Extremity scores (FM-UE) [26].

Table 2.3.1 Stroke Participants Demographics

Subject ID	Lesion Side	Paretic Hand	Race	FM-UE (Total:66)	Stroke Year
S001	Right	Left	White	6	2017
S002	Right	Left	White	63	2019
S003	Left	Right	White	11	2014
S004	Left	Right	White	26	2019
S005	Left	Right	Black or African American	63	2013
S006	Left	Right	White	32	2021
S007	Right	Left	Not Reported	40	2019
S008	Right	Left	Black or African American	19	2021
S009	Left	Right	White	62	2007

Subjects' index fingers were stimulated using Digitimer DS7A Constant Current Stimulator (Digitimer Ltd, Welwyn Garden City, UK). The electrodes were placed with the positive and ground termini on the distal and intermediate phalanges on the index finger, respectively, as displayed in **Figure 2.3.1**. Stimulation was applied first to the paretic and then non-paretic hand in the stroke group to allow for within-subject comparisons. Stimulation was applied to the dominant hand of control participants. The stimulus was delivered in the form of a DC square wave with a duration of 200μs and current normalized to twice the sensation threshold for each participant. Stroke participants had a significantly higher sensation threshold than healthy subjects in their paretic hands (two-sample *t*-test $p = 0.025$), resulting in higher actual stimulation intensity. There was no significant difference in sensation threshold or actual stimulation intensity between the tested hand in healthy controls and the non-paretic hand in stroke. Each trial was one minute in duration, consisting of 120 individual stimuli delivered at 2 Hz, and 5 trials were conducted for each participant.

Brain response data was collected using the BrainVision Recorder EEG System (Brain Vision LLC, Morrisville, NC). An EasyCap electrode cap (EASYCAP GmbH, Woerthsee-Etterschlag, Germany) of the correct size for each participant was fitted with 64 electrodes in the 10-20 system. A sampling rate of at least 1000 Hz was used to collect all data, and a software notch filter was enabled at 60 Hz to mitigate interference by the electrical grid.

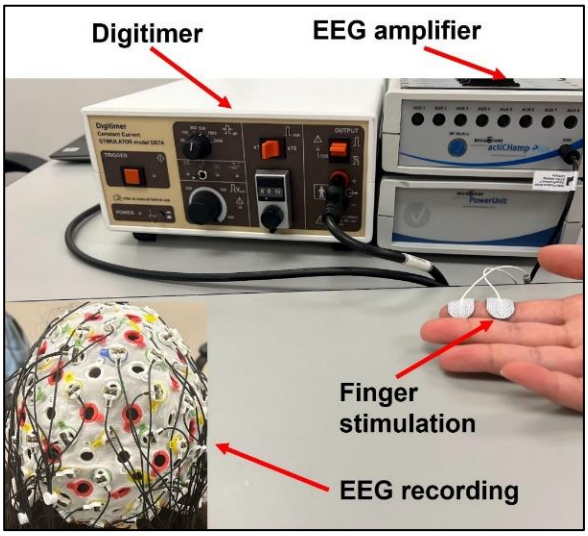

Figure 2.3.1 Experimental Setup

Data analysis was conducted in EEGLAB [64] for MATLAB R2020a (MathWorks, Natick, MA, USA). First, all trials were appended to each other. The data were visually inspected, and noisy or otherwise unsuitable channels were removed. After bandpass filtering between 1 and 45 Hz, each dataset was re-referenced to the global average reference of all remaining channels and epoched with a window of -80 to 300 ms surrounding each stimulus. Epoch baselines were calculated from -80 to 0 ms before the stimulus and removed. A notable artifact of stimulation was observed in each participant along a window from 0 to 2.5 +/- 0.3 ms after stimulus. This unique interval was identified for each participant, both stroke and controls, and replaced with a cubic interpolation of the data for 50 ms on either side of the window.

Epochs were then visually inspected and rejected based on the presence of blinking and movement artifacts, leaving 300 epochs on average per participant. The epochs were then averaged in each participant to extract the somatosensory evoked potentials (SEP). The latency and amplitude of early SEP components, P50 and N100, were measured at both contralateral and

ipsilateral hemispheres around the sensorimotor areas, i.e., C3/4, C5/6, C1/2, CP3/4, CP5/6, CP1/2. For each participant, the latency of each component was taken at the electrode where the amplitude was maximal over each hemisphere, and the amplitude was measured at each electrode over the same hemisphere at that latency. ERP voltage maps were calculated and drawn at the mean latency of each component. The standardized low-resolution electromagnetic tomographic analysis, sLORETA (v20200701) was used to localize the ERP source activity on the cortex [65, 66].

The laterality index was computed to investigate the hemisphere dominance of cortical response in the time window of the P50-N100 [67, 68]. The LI is defined as the signal power difference between contralateral and ipsilateral hemispheres in the sensorimotor areas (including C1/2, C3/4, C5/6, CP1/2, CP3/4, CP5/6 in 10/20 EEG recording system) and then normalized by their sum, as shown in the equation below. A higher LI indicates a stronger contralateral dominance (healthy normal) while a reduced LI indicates either more bilateral activities or an ipsilateral dominance (if LI < 0) that is likely due to functional reorganization in the brain.

$$\mathbf{LI} = \frac{\mathbf{Contralateral} - \mathbf{Ipsilateral}}{\mathbf{Contralateral} + \mathbf{Ipsilateral}} \quad (1)$$

Statistical analyses were performed by commercial software Statistical Analysis Systems (9.4, SAS, Carey, NC, USA). First, an independent *t*-test was performed to ensure the stroke participants and controls had a similar age range (50-80 years, two-sample *t*-test $p = 0.23$). Analysis of variance (ANOVA) was performed to check the statistical significance of the results using stimulation category (stroke paretic vs. stroke non-paretic vs. controls) for ERP latencies, mean amplitudes, and mean laterality index. Then summary statistics were computed including

means, 95% CI, medians, and standard deviations (**Table 2.3.2**). We checked the outcome variables to assure they were normally distributed; and found no evidence to the contrary. We then analyzed the data using correlated data analysis with generalized estimating equations (GEE) (PROC GENMOD) to produce correlated linear models for each outcome variable. We utilized GEE analysis because it offers robust beta estimates despite variance structure specification. Because two of our comparisons were correlated (stroke-involved and stroke uninvolved arms), and one was not (control), this methodology allowed for comparison of the correlated data. We performed separate GEE analyses using the stimulation category (stroke paretic vs. stroke non-paretic vs. controls) for ERP latencies, mean amplitudes, and mean laterality index. We then completed Pearson correlation analyses between ERP latencies and amplitude and motor impairment levels.

Results

Visualization of the contralateral and ipsilateral (to stimulated hand) SEP responses to finger stimulation are shown in **Figures 2.3.2 and 2.3.3**. The contralateral SEPs (P50 and N100) were shown in both stroke and control participants, while the ipsilateral SEPs were mainly shown in stroke participants when their paretic hand was stimulated.

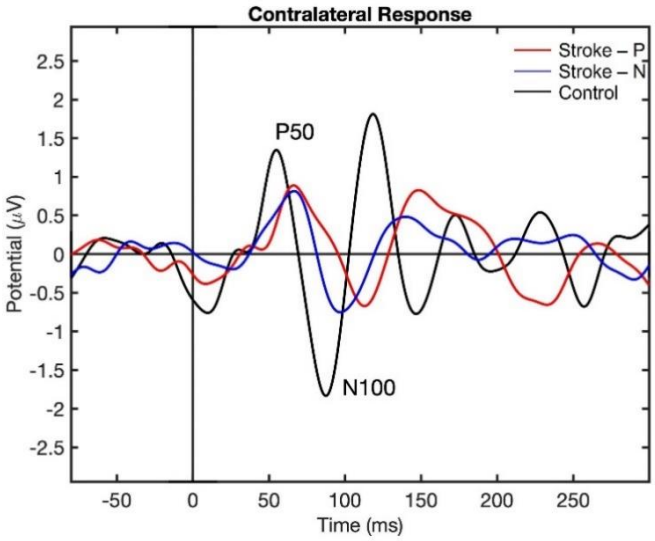

Figure 2.3.2 Contralateral SEP response to finger stimulation. Stroke-P (red): Paretic hand was stimulated. Stroke-N (blue): non-paretic hand was simulated. Control (black): Dominate hand was stimulated.

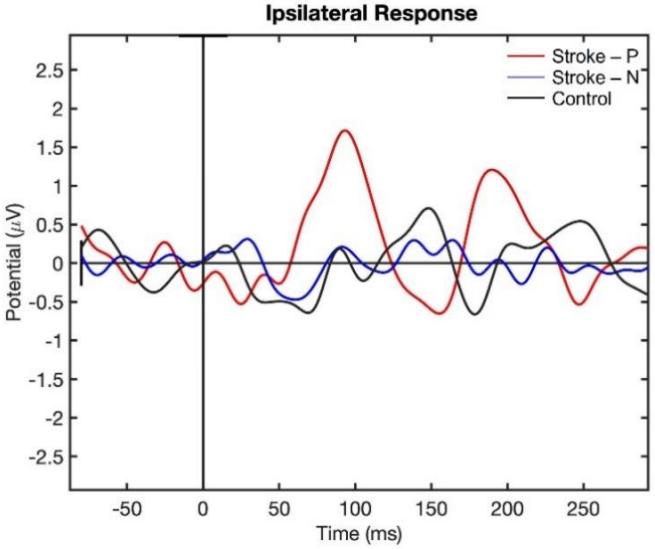

Figure 2.3.3 Ipsilateral SEP response to finger stimulation. Stroke-P (red): Paretic hand was stimulated. Stroke-N (blue): non-paretic hand was simulated. Control (Black): Dominate hand was stimulated.

The descriptive statistics of the latency, amplitude, and laterality index are displayed in **Table 2.3.2**. In the contralateral (to stimulated hand) hemisphere, the ANOVA results showed that the latencies of P50 ($F(2,22) = 12.71$, $p<0.0002$) and N100 ($F(2,22) = 10.06$, $p<0.0008$) were significantly different between groups. Individual GEE analysis showed that the latency of P50 was significantly delayed in both the paretic hand ($z=4.76$, $p=<0.0001$) and the non-paretic hand (P50 $z=3.33$, $p=0.0009$) compared to the controls. Additionally, at timepoint N100, the stroke paretic hand ($z=4.16$, $p=<0.0001$) was significantly delayed compared to controls. For stroke participants, within-subject comparisons show that the latencies of P50 (paretic vs. nonparetic: $z=2.82$, $p = 0.0047$) and N100 ($z=3.44$, $p = 0.0006$) were larger for stimulation at paretic hand than nonparetic (**see Figures 2.3.4 and 2.3.5**).

Table 2.3.2. Descriptive Statistics

Measure	**Mean**	**Mean**	**95% CL lower**	**95% CL higher**	**Std**	**Min**	**Max**	**Median**
Latency								
Latency - P50	Stroke-P	71.30	60.12	82.48	13.37	55.00	93.60	70.10
Latency - P50	Stroke-N	57.51	52.46	62.57	6.58	51.40	67.00	54.00
Latency - P50	Control	49.30	45.89	52.71	4.08	42.00	53.80	51.10
Latency - N100	Stroke-P	134.30	112.63	155.97	25.92	87.00	158.00	149.20
Latency - N100	Stroke-N	99.40	86.11	112.69	17.29	78.00	134.40	96.00
Latency - N100	Control	91.13	76.38	105.87	17.64	72.00	119.00	85.80

Amplitude (Amp)								
Amp. - P50	Stroke-P	0.49	0.23	0.74	0.33	0.00	0.88	0.62
Amp. - P50	Stroke-N	0.75	0.49	1.00	0.33	0.31	1.25	0.69
Amp. - P50	Control	0.75	0.39	1.12	0.44	0.13	1.66	0.69
Amp. - N100	Stroke-P	-0.69	-1.26	-0.12	0.74	-2.28	0.00	-0.39
Amp. - N100	Stroke-N	-0.37	-0.56	-0.17	0.25	-0.85	-0.01	-0.33
Amp. - N100	Control	-0.43	-0.84	-0.02	0.49	-1.28	-0.00	-0.20
Laterality Index (LI)								
Mean LI	Stroke-P	0.56	0.15	0.96	0.48	-0.25	1.00	0.68
Mean LI	Stroke-N	0.93	0.81	1.04	0.15	0.54	1.00	0.98
Mean LI	Control	0.95	0.91	1.00	0.06	0.86	1.00	0.99

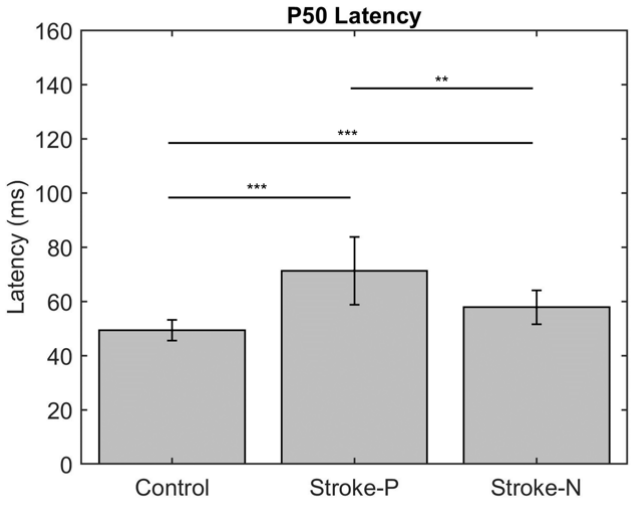

Figure 2.3.4 Latency of Contralateral (to Stimulated Hand) SEP component P50. Stars indicate statistically significant differences between groups (control, stroke paretic hand (Stroke-P) and stroke non-paretic hand (Stroke-N)) *<0.05 **<0.01 ***<0.001

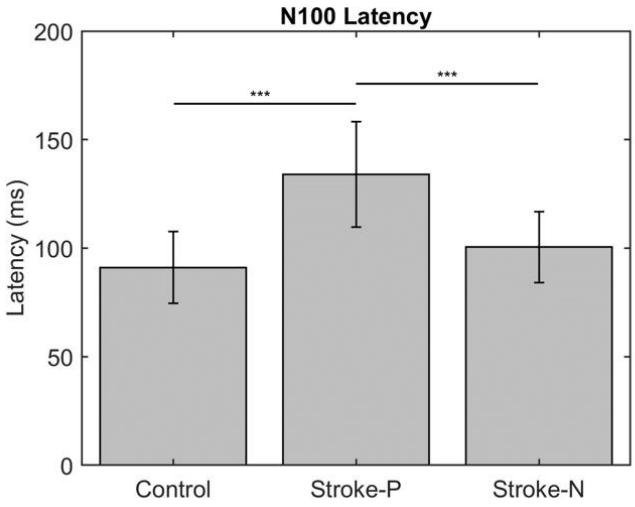

Figure 2.3.5 Latency of Contralateral (to Stimulated Hand) SEP component N100. Stars indicate a statistically significant difference between groups (control, stroke paretic hand (Stroke-P) and stroke non-paretic hand (Stroke-N)): *<0.05 **<0.01 ***<0.001

The amplitude differences of P50 and N100 in the contralateral (to stimulated hand) hemisphere were not statistically significant between stroke and control groups. The mean values of amplitude are reported in **Table 2.3.2**. The Pearson correlation analysis (**see Figure 2.3.6**) showed that there was a significant negative linear relationship between the P50 amplitude of the contralateral (to stimulated hand) SEP responses and Fügl-Meyer Upper Extremity (FM-UE)

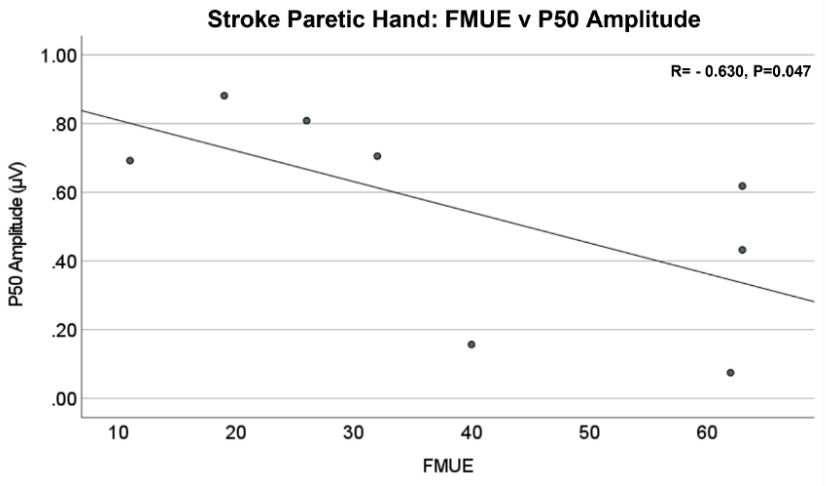

Figure 2.3.6 Stroke Paretic Hand: Fügl-Meyer Upper Extremity (FM-UE) score vs. P50 Amplitude in the Contralateral (to stimulated hand) hemisphere. There is a significant negative linear relationship between P50 amplitude and FM-UE Score (R=-0.630, P=0.047)

Score (R=-0.630, P=0.047). No significant correlations were found between FM-UE and other SEP measures.

The laterality index **(Figure 2.3.7**) was significantly lower when the stroke paretic hand was stimulated compared to the stroke non-paretic hand (z=-2.44, p=0.033) and healthy control (p=0.022), indicating more bilateral or ipsilateral cortical activities after a stroke. This was also evident in source localization results where only contralateral source activity was detected in healthy controls, which was in line with previous findings [69-71], while bilateral source activities were shown in individuals after a stroke **(Figures 2.3.8-10).**

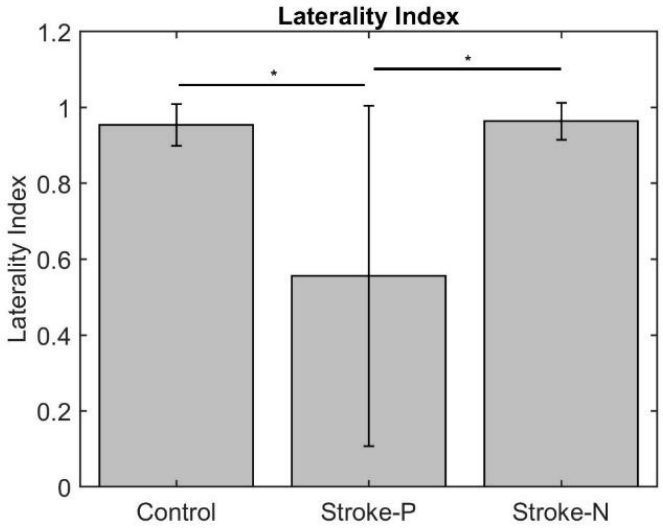

Figure 2.3.7 Laterality Index. Stars indicate statistically significant differences among control, stroke paretic hand (Stroke-P), and stroke non-paretic hand (Stroke-N): *<0.05 **<0.01 ***<0.001

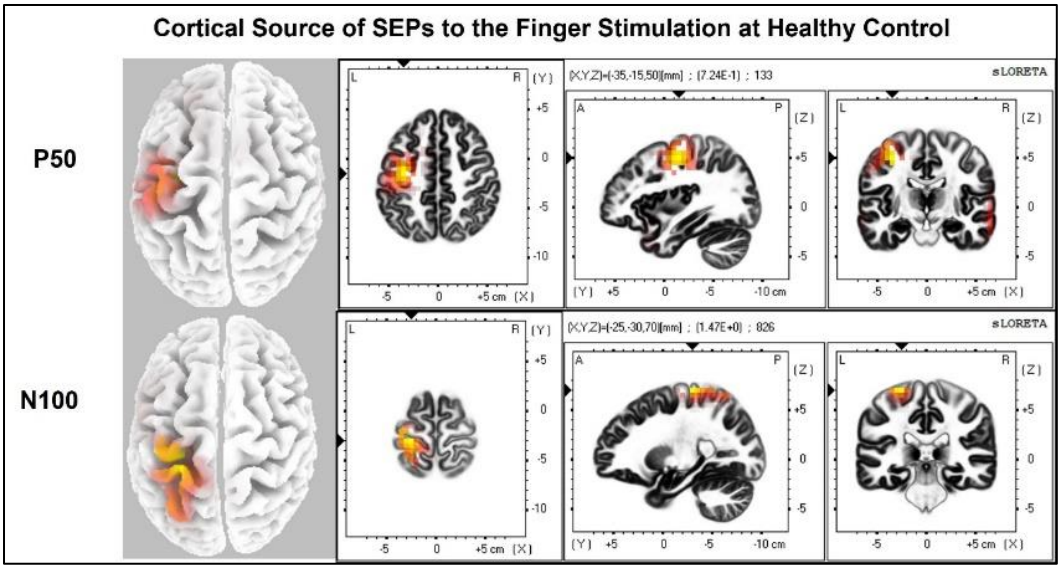

Figure 2.3.8 Cortical sources of SEP components in Healthy Control. The right hand was stimulated, and only contralateral (left) cortical sources were detected for P50 and N100.

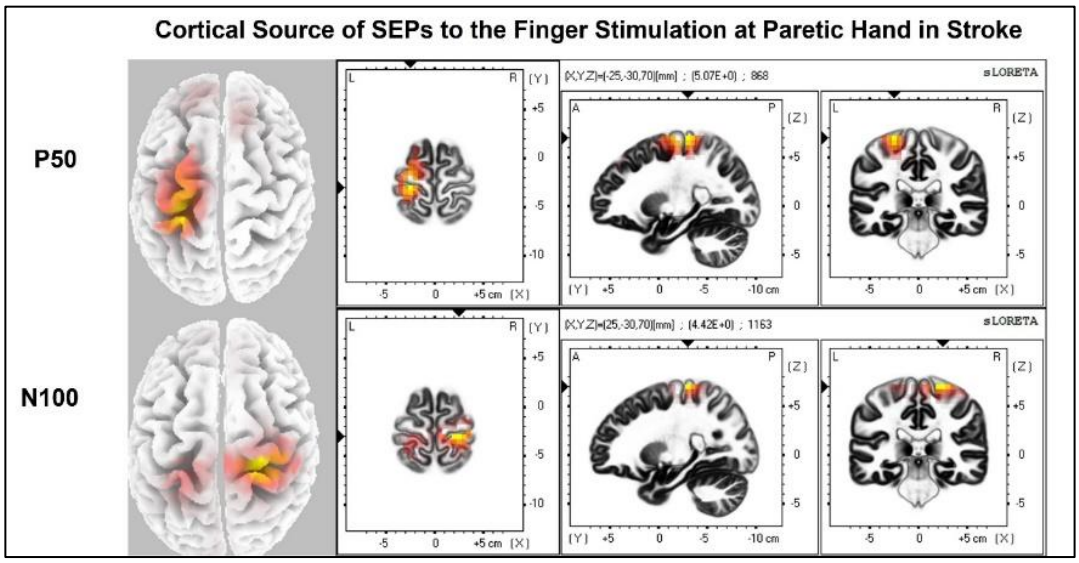

Figure 2.3.9 Cortical sources of SEP components in stroke when the paretic hand is stimulated. The paretic (right) hand was stimulated, contralateral (left) source activities were detected at the time point of P50, and bilateral source activities (more activities in the ipsilateral (right) hemisphere) are detected at the time point of N100.

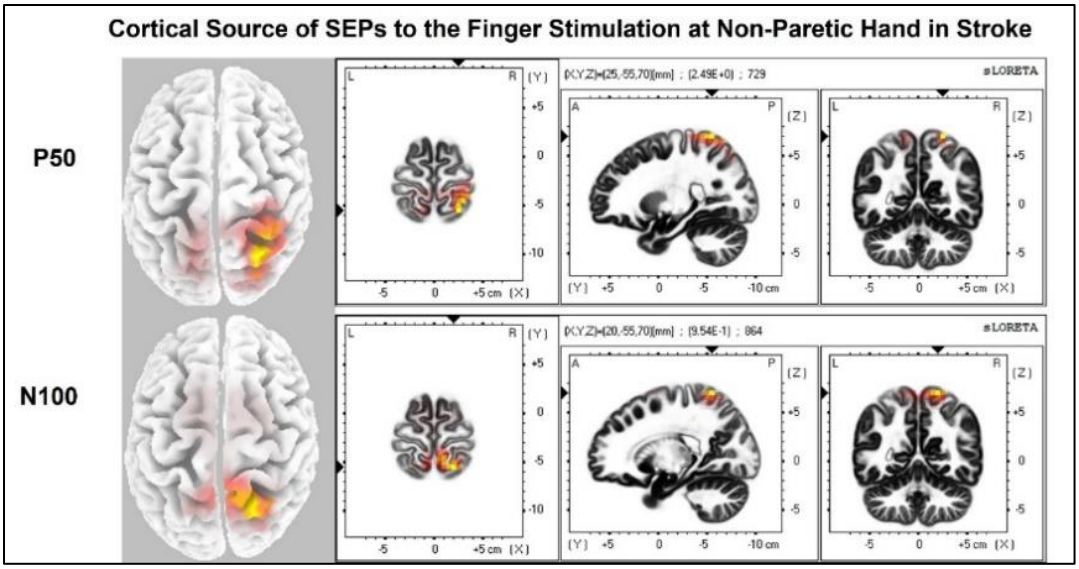

Figure 2.3.10 Cortical sources of SEP components in stroke when the non-paretic hand is stimulated. Non-paretic (left) hand was stimulated, and contralateral (right) source activities were detected mainly at the time points of P50 and N100.

Discussion

The laterality index and source localization results showed that bilateral cortical responses occurred in stroke participants when their paretic hand was stimulated, while controls had only unilateral cortical responses on the contralateral (to stimulated hand) hemisphere. The bilateral response in stroke participants was mostly seen at the timepoint of N100. These results suggest somatosensory reorganization occurs post-stroke. This reorganization is likely due to the increased recruitment of ipsilateral cortical regions during the processing of the somatosensory signals from the paretic hand. This is consistent with neuroimaging studies that have demonstrated increased ipsilateral cortical sensorimotor activity during movement [19, 72-74], which may require the sensory signal to re-route to provide sensory feedback for ipsilateral motor control.

The change in somatosensory neural circuitry might occur subcortically, however, there is no known ascending bilateral or ipsilateral pathway for carrying tactile signals from a distal periphery nerve to the somatosensory cortices. The ascending pathways in the dorsal column that convey tactile sensation from the paretic arm project contralaterally to the primary sensory cortex

in the lesioned hemisphere. Therefore, a potential neural mechanism may be a crossover of signals in the corpus callosum. This would also explain the ipsilesional activity during the P50 and the more delayed contralesional N100 somaesthetic evoked potential following stimulation of the paretic index finger. The corpus callosum is the largest white matter pathway connecting the two cerebral hemispheres and has the role of mediating interhemispheric modulation between the primary motor cortex and sensory cortices to facilitate coordinated movements [75]. The assumption of its role in post-stroke somatosensory processing is based on existing knowledge that interhemispheric transfer of sensory information relies on the posterior half of the corpus callosum and the integrity of the sensory region is reduced in chronic stroke [75-77]. Additionally, other research has shown that bilateral activation of the primary somatosensory cortex occurs during mirror therapy post-stroke and the corpus callosum was found to be involved [78]. This interhemispheric transfer of sensory information can also explain the delayed latency of the N100 SEPs for stimulation of the stroke paretic hand as we reported in this study. The delayed latency at timepoint P50 is likely due to stroke-induced supra-spinal damage of the dorsal columns (white matter stroke) since the source localization results show mostly activation over the lesioned hemisphere.

Additionally, while not statistically significant, the reduced amplitudes are in line with prior studies on SEP's post-stroke [79-81]. The negative linear relationship between P50 amplitude and Fügl-Meyer impairment shows that the degree of the motor impairments is related to the hemispheric shift in cortical responses of sensory information post-stroke. This is consistent with the literature as Keren, Ring [82] established a negative relationship between upper limb SEP with clinical performance. This information on the relationship between the change in SEP and motor impairment is clinically significant. While it is known that somatosensory deficits worsen the

recovery of motor function and adding sensory stimulation in rehabilitation practices enhances motor recovery, sensory reorganization in an injured brain is not sufficiently considered in current clinical practices [83, 84]. This information potentially helps predict the severity of motor impairment based on the degree of cortical activity to sensory stimulation after a stroke. If motor impairment could be gauged from a sensory perspective, this would help complete a more comprehensive assessment, especially in those individuals who can barely perform any upper limb movements. Additionally, directed rehabilitation interventions focusing on engaging the somatosensory tracts have the potential to enhance motor recovery for individuals in the acute/subacute phases of recovery whose movement ability is still limited or absent. This type of directed sensory rehabilitation is currently being explored, such as focal repetitive muscle vibration, which is a non-invasive post-stroke therapy to reduce muscle tone [85, 86]. Another example is wearable focal stimulation devices, such as a vibrotactile glove (VTG), which provides vibratory input to the paretic limb of chronic stroke survivors and has been shown to promote neural plasticity and reduces spasticity [87, 88]. Other studies have used robot-assisted somatosensory training and vibrotactile biofeedback devices [89, 90].

In summary, this research provides new knowledge to further understand neural mechanisms underlying motor deficits induced by somatosensory reorganization after a hemiparetic stroke. This is significant because this will pave the way to provide a sensitive biomarker based on EEG to enrich future science-driven therapeutic rehabilitation strategies from a sensory or sensory-motor perspective, thus improving stroke recovery.

Limitations and Future Work is related to the lack of fine anatomical resolution in the EEG to determine the physical pathway of re-route somatosensory process in the brain, and the limited number of participants. While EEG boasts sufficient temporal resolution to elucidate the delay of

action and reorganization of the somatosensory processing network in impaired stroke patients, it cannot be used to determine which pathway neural signals take from the contralateral to the ipsilateral cortex. Additionally, EEG provides very limited information on any changes in subcortical regions. Therefore, while we assume that the crossover in sensory signals occurs at the corpus callosum, the exact pathway remains hypothetical. Other modalities of neuroimaging, such as functional magnetic resonance imaging (fMRI) or diffusion tensor imagining might offer an improved ability to determine information flow in the brain in real time. In addition, future work could also involve simultaneous EEG-fMRI to provide a more precise interpretation of results. If this relationship is successfully established, it would further our understanding of neuroplasticity following unilateral brain injury. This would aid in improved rehabilitation strategies such as neurostimulation, which to this point has found very limited clinical adoption given its temporary effects. An additional aspect of this study that could be improved is the small sample size. Therefore, future work will focus on increasing the number of study participants.

Chapter 3: Identify Sex-Specific Imaging Biomarkers for Mild Cognitive Impairment and Alzheimer's Disease

3.1 Background

Dementia is the loss of cognitive function to such an extent that it interferes with daily life and activities. Alzheimer's disease (AD) is the most common form of dementia among older adults and is characterized by amyloid plaques, neurofibrillary tau, and loss of connection between neurons in the brain [91, 92]. The National Institute of Health estimates the prevalence of AD in individuals 65 years or older in the United States is approximately 6.5 million, and this number is projected to increase to 13.8 million by the year 2060. AD is currently the fifth leading cause of death for those older than 65 years living in the United States [93, 94]. The symptoms of AD include memory loss, poor judgement, confusion, difficulty speaking, reading, or writing, and obsessive, repetitive, or impulsive behavior [91]. The study of AD is critically important, not only because the disease causes a significant loss of function, but because the cost of caring for an individual diagnosed with AD during the last five years of life has been estimated at $287,000 [95].

In recent years, research in the molecular pathogenetic events associated with AD has made tremendous progress, however the cause of AD is still unknown and there is currently no curative treatment options available [96]. The studies on AD risk factors have found that AD is not primarily a disease linked directly to defective genes, but a complex syndrome dependent on the rate of aging and influenced by many genetic and environmental risk factors and the general health of the patient [97]. Due to this complexity, precision medicine techniques have been of interest for the study of Alzheimer's Disease treatments [98, 99]. Importantly, disrupted connection between neuronal populations fundamental for higher order cognitive processing and memory have been

implicated. Network studies have shown that AD has global brain connectivity differences, and this pathology is not equally distributed, but preferentially affects specific hub areas [100, 101]. Specifically, selective disruption has been found in the posterior and parietal hubs, left temporal centrality, and the hippocampus [102, 103]

Alzheimer's Disease disproportionately affects females as they constitute more than two-thirds of the AD population [104]. The higher prevalence of AD in females has been attributed to females having greater longevity compared to males [105]. Since age is the greatest risk factor for the development of AD, it would be reasonable to state that more females would live long enough to develop AD. However, increasing evidence suggests there are other factors that contribute to the sex-specific risk of AD. This difference has been attributed to a variety of sex-specific factors including genetics (such as the presence of the 'X' chromosome [106]), hormonal differences and menopause, and hypertensive disorders of pregnancy [107-110]. As well as known risk factors depression, education level, sleep differences, and genetics (such as apolipoprotein E4 [111]) [105, 109]. In addition to prevalence differences, females experience greater cognitive deterioration than males in the same disease stage [112] that are also present in individuals with MCI [113]. Compared to males with AD, females perform worse on a variety of neuropsychological tasks and have greater total brain atrophy and temporal lobe degeneration [114-116].

Recently, research has revealed that brain imaging markers may also be a contributing factor in sex differences, specifically related to the hippocampus [117]. The damage demonstrated in the AD brain initially occurs in the entorhinal cortex and hippocampus, areas of the brain largely impacting cognition, particularly memory. Individuals diagnosed with early AD or mild cognitive insufficiency (MCI), have a reduction in their hippocampal volume, combined with

microhemorrhage [118, 119]. Additionally, hippocampal atrophy has been found to be significantly faster and affect the progression of AD only in females [120, 121]. Researchers have found that males have a higher anterior cingulate cortex amyloid load and glucose hypometabolism in the precuneus, posterior cingulate, and inferior parietal cortex [122]. Similar findings have been reported among cognitively normal adults suggesting that males have a higher brain resilience [123].

Therefore, the work of this section focuses on finding sex differences in brain functional connectivity of the hippocampus in MCI and AD. The goal of this work is to hopefully aid in the development of sex-specific treatments to increase more favorable outcomes as the interventions could be targeted to address individualized risks.

3.2 Aging Study 1: Identify Sex-Specific Imaging Biomarkers for Mild Cognitive Impairment

Objectives

Mild cognitive impairment (MCI) always precedes AD, usually years before meeting the diagnostic criteria of clinical dementia and is the most important predictor of AD [124]. MCI is defined as cognitive decline greater than expected for a given age but does not notably interfere with daily activities [125]. Current clinical evidence demonstrates about a 20% annual conversion rate of MCI to AD and that more than half of the individuals with MCI progress to dementia within five years [126-129]. The hippocampus is also known to be affected at the earliest stages of MCI, even before a diagnosis can be made [130]. Recent research revealed additional brain imaging markers that may also contribute to the sex differences in AD and are specifically present in individuals with MCI and that reduced hippocampal volume and any microhemorrhage, regardless of location, are the best MRI features to predict the transition from pre-MCI to MCI However, the

role of sex-related differences in hippocampal connectivity during MCI has not been elucidated yet.

This study was designed to extend the understanding of the mechanism underlying the sex differences in pathophysiological biomarkers in individuals with MCI. Our hypothesis was that hippocampal functional connectivity (FC) to the precuneus cortex and the brain stem shows sex- and MCI-specific differences. The FC of the hippocampus will be analyzed and compared between females and males with MCI, as well as cognitively normal females and males as controls.

Methods

The data for this study were extracted from the ADNI [131], which is a publicly accessible dataset available at adni.loni.usc.edu. Launched in 2003, ADNI is a longitudinal, multi-site, cohort study, led by Principal Investigator Michael W. Weiner, MD. The original study, ADNI-1, has been extended three times and the database contains subject data from ADNI-1, ADNI-GO, ADNI-2, and ADNI-3. The overall goal of the studies was to evaluate whether serial magnetic resonance imaging (MRI), positron emission tomography (PET), other biological markers, and clinical and neuropsychological assessment can be combined to measure the progression of mild cognitive impairment (MCI) and early Alzheimer's disease (AD). For up-to-date information, see www.adni-info.org.

The data were screened for subjects with MCI. To eliminate multiple images from the same subject, the data included early MCI (EMCI), late MCI (LMCI), or MCI from the 1-year subject visit of ADNI-1, ADNI-GO, ADNI-2, and ADNI-3. Subjects' selection was also limited to those with data collected from resting-state functional magnetic resonance imaging (rs-fMRI) and 3.0-Tesla T2 magnetic resonance imaging. A similar search methodology was applied for cognitively

normal (CN) subjects. The screening resulted in a total of 40 MCI females, 42 MCI males, 25 CN females, and 20 CN males. To balance the number of subjects in each group, 20 of each group were randomly selected for the study. Demographics of MCI subjects are provided in **Table 3.2.1**. This includes age, Apolipoprotein E (ApoE) genotype, the Mini Mental State Examination (MMSE), the Geriatric Depression (GD) Scale, the Global Clinical Dementia Rating (CDR), and the Functional Activities Questionnaire (FAQ), and the Neuropsychiatric Inventory Questionnaire (NPI-Q). IBM SPSS (IBM Corp. Armonk, NY, USA) was used to run independent t-tests to ensure there was not a statistically significant sex difference in age, MMSE, GD Scale, CDR, FAQ and NPI-Q ($P > 0.05$). If normal distribution could not be assumed based on the Shapiro-Wilk test, a non-parametric Mann-Whitney test was performed. These values are provided in **Table 3.2.1**.

Table 3.2.1 Mild Cognitive Impairment Subject Demographics

ID	Sex	Age	ApoE genotype	MMSE	GD Scale	CDR	FAQ	NPI-Q
S001	F	74	ε3 ε3	26	6	0.5	0	3
S002	F	65	ε4 ε4	25	1	0.5	1	1
S003	F	71	ε4 ε4	29	0	0.5	0	0
S004	F	80	ε3 ε3	25	1	0.5	0	1
S005	F	70	ε3 ε3	30	5	0.5	0	-
S006	F	65	ε4 ε4	27	7	1.0	30	10
S007	F	79	ε3 ε3	29	0	0.5	4	2
S008	F	58	ε3 ε4	30	1	0.5	0	3
S009	F	76	ε3 ε4	26	7	0.5	4	8
S010	F	61	ε3 ε3	29	3	0.5	5	0
S011	F	72	ε3 ε4	28	2	1.0	19	16
S012	F	72	ε3 ε3	28	5	0.5	0	0
S013	F	84	ε3 ε3	28	6	0.5	8	0
S014	F	69	ε3 ε3	26	1	0.5	0	0
S015	F	72	ε3 ε3	30	2	0.5	0	3
S016	F	72	ε3 ε4	28	0	0.5	6	4
S017	F	81	ε3 ε4	25	2	0.5	7	3
S018	F	77	ε3 ε3	29	1	0.5	0	2
S019	F	67	ε3 ε3	29	2	0.5	0	0
S020	F	63	ε3 ε3	29	1	0.5	1	1
S021	M	68	ε3 ε4	29	0	0.5	2	3

S022	M	72	ε3 ε4	29	0	0.5	12	4
S023	M	62	ε4 ε4	29	0	0.5	0	0
S024	M	58	ε3 ε3	25	0	0.5	1	2
S025	M	74	ε3 ε4	28	2	0.5	3	2
S026	M	63	ε2 ε3	30	1	0.5	1	2
S027	M	90	ε3 ε3	26	2	0.5	4	11
S028	M	86	ε3 ε3	25	1	0.5	6	3
S029	M	87	ε3 ε4	29	1.	1.0	10	12
S030	M	70	ε2 ε4	28	2	0.5	2	8
S031	M	74	ε2 ε3	30	3	0.5	0	2
S032	M	75	ε3 ε4	27	5	1.0	21	7
S033	M	69	ε3 ε3	27	1	0.5	0	1
S034	M	74	ε3 ε3	29	2	1	0	0
S035	M	77	ε2 ε3	28	6	0.5	7	8.0
S036	M	80	ε3 ε4	21	3	1.0	22	4
S037	M	73	ε3 ε4	30	2	0.5	2	2
S038	M	76	ε3 ε3	30	1	0.5	1	1
S039	M	62	ε4 ε4	27	5	0.5	3	7
S040	M	76	ε3 ε3	23	5	0.5	3	4
Female μ ± SD		**71±7.1**	-	**27.7±1.7**	**2.5±2.4**	**.55±.16**	**4.4±7.7**	**3.0±4.1**
Male μ ± SD		**73±8.5**	-	**27.5±2.5**	**2.1±1.9**	**0.6±.21**	**5.0±6.5**	**4.1±3.5**
Between sex t-tests		**P=0.44**	-	**P=0.95**	**P=0.58**	**P=0.38**	**P=0.22**	**P=0.12**

The subject's original rs-fMRI and MRI images (NiFTI format) were imported into the NITRC Functional Connectivity Toolbox (CONN) version 20b [132]. CONN utilizes SPM12 (Welcome Department of Cognitive Neurology, UK) and MATLAB R2020a (MathWorks, Natick, MA, USA) in its processes and by default a combination of the Harvard-Oxford atlas (HOA distributed with FSL http://www.fmrib.ox.ac.uk/fsl/) [133-135] and the Automated Anatomical Labeling (AAL) atlas [136].

The images were processed through the default functional and structural preprocessing pipeline as detailed in [137]. This included realignment, slice timing correction, coregistration/normalization, segmentation, outlier detection, and smoothing. Additionally, this

step extracted the blood-oxygen-level dependent (BOLD) time series from the regions of interest (ROIs) and at the voxels. Next, the images were denoised to remove confounding effects from the BOLD signal through linear regression and band-pass filtering. A quality assurance check was made after the denoising to ensure normalization and that there were no visible artifacts in the data.

A seed-to-voxel analysis was conducted for each subject. This analysis created a seed-based connectivity (SBC) map between the ROI (left or right hippocampus) to every voxel of the brain. The SBC map is computed as the Fisher-transformed bivariant correlation coefficients between the ROI BOLD time series and each individual voxel BOLD time series [138]. The mathematical relationship to construct the SBC is shown below.

$$r(x) = \frac{\int S(x,t)R(t)dt}{(\int R^2(t)dt \int S^2(x,t)dt)^{1/2}}$$

$$Z(x) = tanh^{-1}(r(x))$$

where R is the average ROI BOLD timeseries, S is the BOLD timeseries at each voxel, r is the spatial map of Pearson correlation coefficients, and Z is the SBC map of the Fisher-transformed correlation coefficients for the ROI. Finally, *F*-tests were conducted between the SBC maps to compare differences between groups. For a cortical area to be considered significant, the toolbox used the Gaussian Random Field theory parametric statistics, with a cluster threshold $p<0.05$ (FDR-corrected) and voxel threshold $p<0.001$ (uncorrected) to control the type I error in multiple comparisons [139]. Additionally, the area must have been over 800 voxels large or cover more than 80 percent of a given atlas (specific brain area).

Results

The brain regions identified to be significantly different between the MCI and CN groups are shown in **Table 3.2.2**. The left and right para hippocampal gyrus, hippocampus, and amygdala all had significant between-group differences in both sexes. The regions that had a sex-specific were the Precuneus Cortex and the Brainstem, observed only in males.

Table 3.2.2 Brain Regions with a Significant Difference between Mild Cognitive Impairment and Cognitively Normal for Each Sex.

Sex	ROI	Brain Area (Atlas)	% Atlas Covered	# Of Voxels
Female (FMCI v FCN)	Right Hippocampus	Left Posterior Para Hippocampal Gyrus	89%	346
		Right Posterior Para Hippocampal Gyrus	89%	283
		Right Hippocampus	100%	342
		Left Hippocampus	94%	318
		Right Amygdala	100%	342
		Left Amygdala	97%	318
	Left Hippocampus	Left Posterior Para Hippocampal Gyrus	91%	354
		Right Posterior Para Hippocampal Gyrus	90%	288
		Right Hippocampus	98%	684
		Left Hippocampus	100%	761
		Right Amygdala	94%	322
		Left Amygdala	100%	327
		Brain Stem	24%	1001
		Precuneus Cortex	18%	993
		Left Posterior Para Hippocampal Gyrus	97%	380

Male (MMCI v MCN)	Right Hippocampus	Right Posterior Para Hippocampal Gyrus	97%	308
		Right Hippocampus	98%	685
		Left Hippocampus	100%	760
		Right Amygdala	100%	342
		Left Amygdala	100%	327
	Left Hippocampus	Brain Stem	20%	829
		Precuneus Cortex	20%	1132
		Left Posterior Para Hippocampal Gyrus	92%	358
		Right Posterior Para Hippocampal Gyrus	94%	299
		Right Hippocampus	98%	685
		Left Hippocampus	100%	760
		Right Amygdala	99%	337
		Left Amygdala	100%	327

In MCI, males showed significantly stronger connectivity of the right or left hippocampus to the left or right precuneus cortex, respectively. This difference is shown visually by comparing boxes A and D in **Figures 3.2.1 and 3.2.2**. There was also a sex specific difference detected in the brain stem. This is visualized in **Figure 3.2.3.**

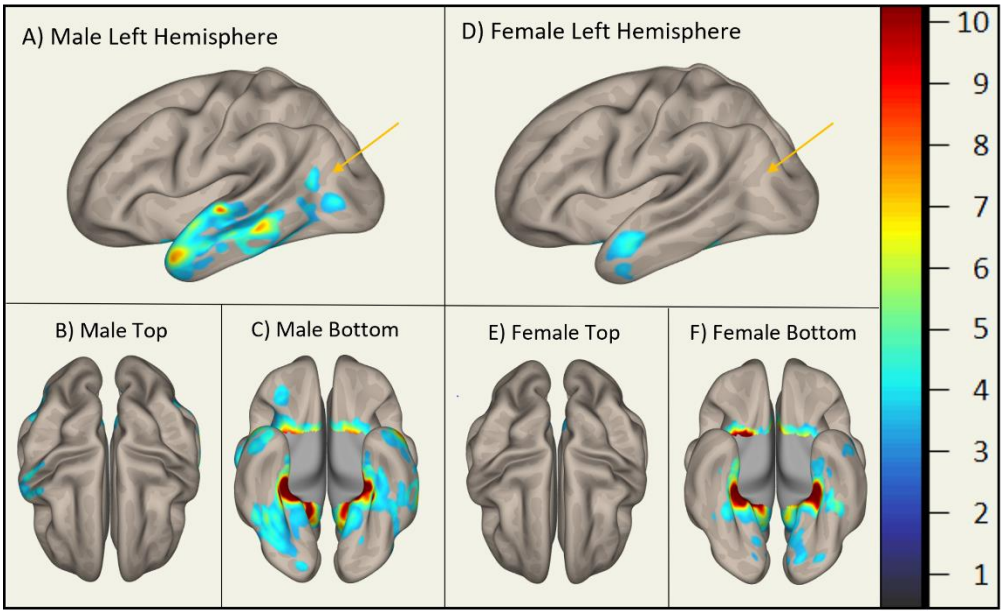

Figure 3.2.1 Sex-Specific Pathological Features with Right Hippocampus as ROI. Highlighted display the statistically significant cortical regions between mild cognitive impairment (MCI) and cognitively normal (CN) ($p<0.001$) normalized to a 1-10 scale. Orange arrows indicate the areas of difference at the precuneus cortex. **A**, **B**, and **C** display MMCI v MCN. **D**, **E**, and **F** display FMCI v FCN

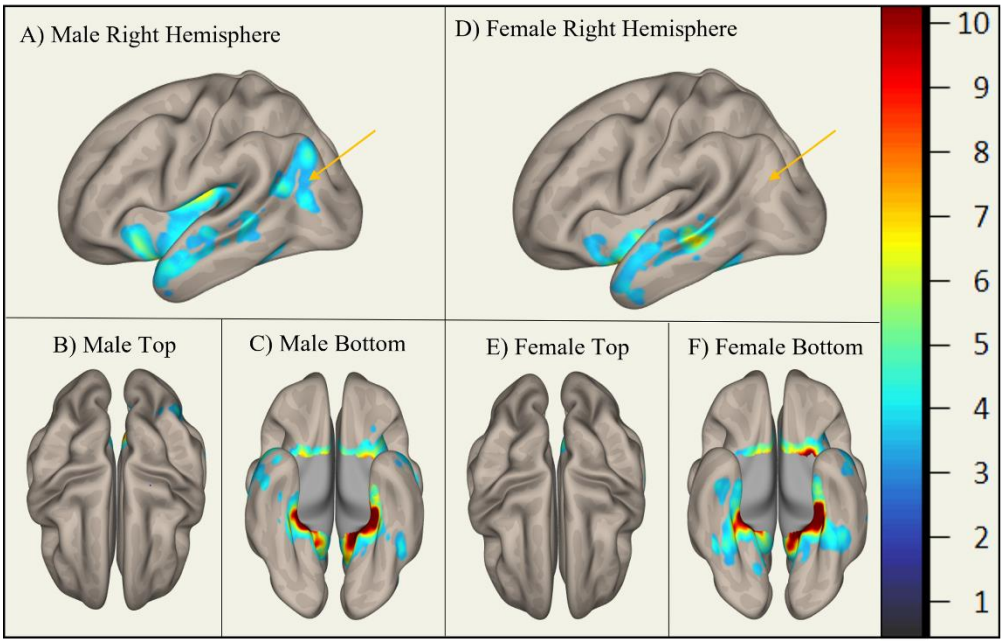

Figure 3.2.2 Sex-Specific Pathological Features with Left Hippocampus as ROI. Highlighted areas display the statistically significant cortical regions between mild cognitive impairment (MCI) and cognitively normal (CN) ($p<0.001$) normalized to a 1-10 scale. Orange arrows indicate the area of difference at the precuneus cortex. **A**, **B**, and **C** display MMCI v MCN. **D**, **E**, and **F** display FMCI v FCN.

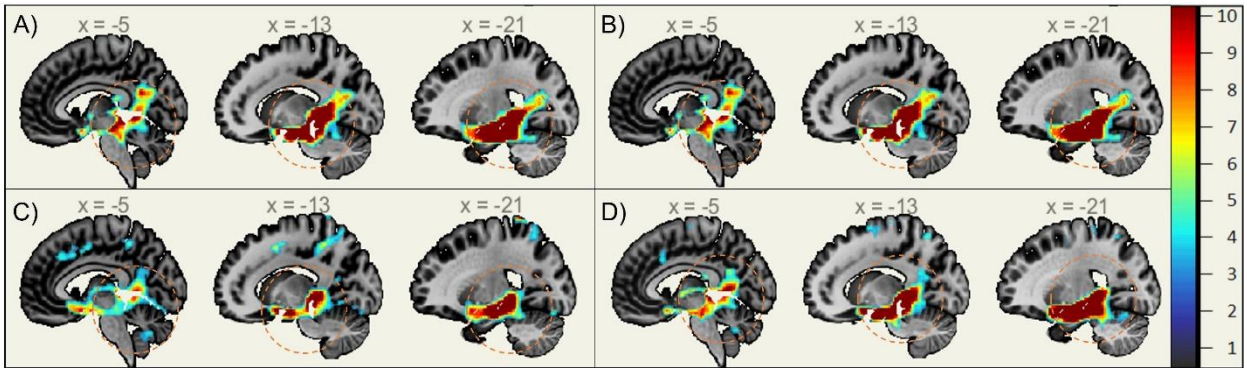

Figure 3.2.3 Sex-Specific Pathological Features Sagittal View. Highlighted Areas display the statistically significant regions between cognitively normal (CN) and mild cognitive impairment (MCI) ($p<0.001$) normalized to a 1-10 scale. Orange circles indicate the area of difference in the brain stem and provide size reference between subplots. **A)** Right Hippocampus ROI MMCI v MCN. **B)** Left Hippocampus ROI MMCI v MCN. **C)** Right Hippocampus ROI FMCI v FCN **D)** Left Hippocampus ROI FMCI v FCN

Discussion

This study supports that there are sex differences in pathophysiological biomarkers of the brain in MCI. Specifically, it extends our current understanding of the role of the hippocampus in these differences. We demonstrate that hippocampal functional connectivity differs to the precuneus cortex and the brain stem between males and females.

The differences found between the MCI and cognitively normal groups across sexes (posterior para hippocampal gyrus, hippocampus, and amygdala) are consistent with prior studies. The posterior para hippocampal gyrus is the cortical ridge in the medial temporal lobe. It contains the hippocampus (covering it medially) and amygdala (covering it anteromedially) [140]. These structures are highly integrated and significant in the process of associative memory [141]. It has been shown that functional connectivity between the hippocampus and amygdala to different regions of the brain is disrupted in MCI [142, 143]. This is consistent with our findings.

The role of the precuneus cortex is consistent with other literature highlighting its importance in the development of AD. The precuneus cortex is in the posteromedial portion of the

parietal lobe. This area has a central role in a wide range of integrated tasks, including visuo-spatial imagery, episodic memory retrieval, and self-processing operations [144]. The precuneus cortex has been shown to have significantly greater activation in MCI, compared to controls, during visual encoding memory tasks [145]. Prior studies have shown that functional connectivity between the hippocampus and precuneus cortex differs between individuals with early AD and healthy controls [146, 147]. However, these studies do not extend to differences between sexes. It has been shown that in individuals with subjective memory complaints, males compared to females had glucose hypometabolism in the precuneus cortex [122]. Our findings extend this knowledge of differences between males and females in the precuneus cortex and show that the effect of MCI on the hippocampal-precuneus cortex functional connectivity may be contributing to the high prevalence of MCI in females.

Previous studies observed that functional connectivity of the locus coeruleus (LC) and the ventral tegmental area (VTA) in the midbrain of the brain stem differ in individuals with AD and MCI. Specifically, the connectivity between the VTA and the para hippocampal gyrus and cerebellar vermis were associated with the occurrence of neuropsychiatric symptoms of AD [148]. Other studies showed that reduced connectivity between the LC and para hippocampal gyrus in MCI was correlated with memory performance [149]. The difference in functional connectivity seen between males and females in this study extends these known connectivity differences seen between MCI and controls to an additional sex difference. This may be a factor in the observed worse neuropsychological tasks seen in females.

The sex differences observed in MCI have also been attributed to other factors besides functional connectivity. For example, cognitive reserve, referring to education and premorbid intelligence (IQ), is associated with the progression of MCI to AD [150]. Furthermore, Giacomucci

et al. reported that sex interacts with cognitive reserve and influences the onset and severity of subjective cognitive decline [151]. Additionally, sex differences in the progression of AD from MCI have been correlated with the ApoE ε4 allele, a well-known risk factor for AD. It has been observed that ApoE ε4 is only significantly correlated to the progression of AD in females [152].

In summary, these findings are significant as they expand our current understanding of the role of the hippocampus-precuneus cortex and hippocampus-brainstem connectivity in sex differences in MCI. Understanding these sex differences in pathophysiology may aid in the development of sex-specific precision medicine to manipulate hippocampal-precuneus cortex and hippocampal-brainstem connectivity to decrease the progression of MCI to AD. Our findings provide the rationale for sex-specific interventions such as cognitive training [153] and neuro-navigation guided, targeted non-invasive brain stimulation [25, 154] or their combination [155].

Limitations and Future Work are related to this study's number of subjects. While this research provides preliminary findings on sex differences in functional connectivity of the hippocampus in individuals with MCI, the small sample size (n=80) is a limitation. Therefore, future work includes increasing sample size in a larger database, as well as expanding functional connectivity from other regions of interest for MCI, in addition to the hippocampus. Furthermore, studies such as these could be furthered by combining mentioned risk factors such as cognitive reserve or genetic differences to explore if there is any connection.

3.3 Aging Study 2: Identify Sex-Specific Imaging Biomarkers for Alzheimer's Disease

Objectives

As previously demonstrated, the functional connectivity from the hippocampus to the precuneus cortex and brain stem was significantly stronger in males than in females in MCI [156].

The aim of this study was to extend this to individuals with AD, to determine if these potential sex-specific functional connectivity biomarkers extend through different disease stages. Using a similar protocol to the previous study, the purpose of our current study is to investigate what differences exist in the functional connectivity of the hippocampus to the rest of the brain in individuals with Alzheimer's Disease.

Methods

The data for this study were extracted from the ADNI [157], which is a publicly accessible dataset available at http://adni.loni.usc.edu. Launched in 2003, ADNI is a longitudinal, multi-site, cohort study, led by Principal Investigator Michael W. Weiner, MD. The original study, ADNI-1, has been extended three times and the database contains subject data from ADNI-1, ADNI-GO, ADNI-2, and ADNI-3. The overall goal of the studies was to evaluate whether serial magnetic resonance imaging (MRI), positron emission tomography (PET), other biological markers, and clinical and neuropsychological assessment can be combined to measure the progression of mild cognitive impairment (MCI) and early Alzheimer's disease (AD). For up-to-date information, see www.adni-info.org.

The data were filtered for participants with AD. Participant selection was limited to those with data collected from resting-state functional magnetic resonance imaging (rs-fMRI) and 3.0-Tesla T2 magnetic resonance imaging. To maximize the sample size, participants were selected from any visit of ADNI-1, ADNI-GO, ADNI-2, and ADNI-3. A similar search methodology was applied for cognitively normal (CN) participants. The screening resulted in a total of 19 AD females, 16 AD males, 33 CN females, and 25 CN males. To balance the number of participants in each group, 16 of each group were randomly selected for the study. Demographics of AD

participants are provided in **Table 3.3.1**; some participants did not have all demographics in the database.

The participant's original rs-fMRI and MRI images (NiFTI format) were imported into the NITRC Functional Connectivity Toolbox (CONN) version 20b [132]. CONN utilizes SPM12 (Welcome Department of Cognitive Neurology, UK) and MATLAB R2020a (MathWorks, Natick, MA, USA) in its processes and by default a combination of the Harvard-Oxford atlas (HOA distributed with FSL http://www.fmrib.ox.ac.uk/fsl/) [133-135] and the Automated Anatomical Labeling (AAL) atlas [136].

The images were processed through the default functional and structural preprocessing pipeline as detailed by Nieto-Castanon [137]. This included realignment, slice timing correction, coregistration/normalization, segmentation, outlier detection, and smoothing. Additionally, this step extracted the blood-oxygen-level dependent (BOLD) time series from the regions of interest (ROIs) and at the voxels. Next, the images were denoised to remove confounding effects from the BOLD signal through linear regression and band-pass filtering. A quality assurance check was made after the denoising to ensure normalization and that there were no visible artifacts in the data.

A seed-to-voxel analysis was conducted for each participant. This analysis created a seed-based connectivity (SBC) map between the ROI (left or right hippocampus) to every voxel of the brain. The SBC map is computed as the Fisher-transformed bivariant correlation coefficients between the ROI BOLD time series and each individual voxel BOLD time series [138]. The mathematical relationship to construct the SBC is:

$$r(x) = \frac{\int S(x,t)R(t)dt}{(\int R^2(t)dt \int S^2(x,t)dt)^{1/2}}$$

$$Z(x) = tanh^{-1}(r(x))$$

where *R* is the average ROI BOLD timeseries, *S* is the BOLD timeseries at each voxel, *r* is the spatial map of Pearson correlation coefficients, and *Z* is the SBC map of the Fisher-transformed correlation coefficients for the ROI.

IBM SPSS (IBM Corp. Armonk, NY, USA) was used to run independent t-tests on the available AD participant data to ensure there was not a statistically significant sex difference in age, the Mini Mental State Examination (MMSE), the Geriatric Depression (GD) Scale, the Global Clinical Dementia Rating (CDR), the Functional Activities Questionnaire (FAQ), and the Neuropsychiatric Inventory Questionnaire (NPI-Q) ($p > 0.05$). If normal distribution could not be assumed based on the Shapiro-Wilk test, a non-parametric Mann-Whitney test was performed.

F-tests were conducted between the SBC maps to compare differences between groups. For a cortical area to be considered significant, the toolbox used the Gaussian Random Field theory parametric statistics, with a cluster threshold $p<0.05$ (FDR-corrected) and voxel threshold $p<0.001$ (uncorrected) to control the type I error in multiple comparisons [139]. Additionally, the area must be over 100 voxels large or cover more than 80 percent of a given atlas (specific brain area).

IIIb Results

Table 3.3.1 displays AD participant demographics with statistical analysis to ensure there were not significant differences in covariates.

Table 3.3.1 Alzheimer's Disease Subject Demographics

ID	Sex	Age	ApoE genotype	MMSE	GD Scale	CDR	FAQ	NPI-Q
S001	F	71.9	ε3 ε4	-	-	-	-	-

S002	F	74.4	ε3 ε3	-	-	-	-	-
S003	F	68.9	ε3 ε4	18.0	1.0	1.0	19.0	2.0
S004	F	60.7	ε3 ε3	-	-	-	-	-
S005	F	75.5	ε3 ε4	24.0	-	1.0	15.0	7.0
S006	F	73.7	ε3 ε4	15.0	1.0	1.0	26.0	3.0
S007	F	58.8	ε4 ε4	18.0	7.0	1.0	25.0	10.0
S008	F	81.8	ε3 ε4	23.0	1.0	1.0	21.0	4.0
S009	F	77.8	ε3 ε4	22.0	2.0	0.5	14.0	9.0
S010	F	74.2	ε4 ε4	26.0	0.0	0.5	6.0	5.0
S011	F	75.9	ε4 ε4	23.0	2.0	1.0	20.0	2.0
S012	F	56.5	ε3 ε4	26.0	1.0	1.0	16.0	2.0
S013	F	87.2	ε3 ε4	19.0	0.0	1.0	28.0	2.0
S014	F	62.8	ε3 ε3	-	-	-	-	-
S015	F	74.9	-	-	-	-	-	-
S016	F	73.6	ε3 ε4	16.0	0.0	1.0	20.0	5.0
S017	M	60.7	ε3 ε3	-	-	-	-	-
S018	M	72.8	ε3 ε4	16.0	2.0	1.0	20.0	7.0
S019	M	77.1	ε3 ε4	25.0	3.0	1.0	20.0	2.0
S020	M	74.3	ε3 ε3	-	-	-	-	-
S021	M	68.8	ε2 ε3	-	-	-	-	-
S022	M	71.9	ε3 ε3	22.0	3.0	1.0	23.0	7.0
S023	M	76.9	ε4 ε4	25.0	1.0	0.5	2.0	0.0
S024	M	79.6	ε2 ε3	21.0	2.0	0.5	9.0	1.0
S025	M	75.9	ε3 ε4	21.0	1.0	1.0	26.0	4.0
S026	M	76.6	ε4 ε4	21.0	4.0	1.0	20.0	14.0
S027	M	66.6	-	-	-	-	-	-
S028	M	75.1	ε4 ε4	23.0	1.0	2.0	22.0	12.0
S029	M	71.6	ε3 ε4	24.0	3.0	1.0	14.0	2.0
S030	M	83.0	ε3 ε4	22.0	1.0	0.5	6.0	1.0
S031	M	80.0	ε3 ε4	23.0	1.0	0.5	9.0	1.0
S032	M	73.9	ε4 ε4	24.0	2.0	1.0	18.0	3.0
Female μ ± SD		**72.8 ± 9.4**	**-**	**20.6 ± 3.9**	**1.5 ± 2.1**	**0.9 ± 0.21**	**19.5 ± 6.4**	**4.4 ± 3.0**
Male μ ± SD		**76.2 ± 3.5**	**-**	**22.3 ± 2.5**	**2.0 ± 1.0**	**0.9 ± 0.42**	**15.7 ± 7.8**	**4.5 ± 4.6**
Between sex t-tests		**P=0.372**	**-**	**P=0.329**	**P-=0.085**	**P=0.740**	**P=0.265**	**P=0.418**

The brain regions identified to be significantly different between the AD and CN groups are shown in **Table 3.3.2**. When the right and left hippocampus were selected as the ROI, the functional connectivity throughout the right and left hippocampus, respectively, had a significant

between-group difference. The regions that had a sex-specific difference were the left and right hippocampus when the right and left hippocampus were selected as ROI, respectively.

Table 3.3.2 Brain Regions with a Significant Difference between Alzheimer's Disease and Cognitively Normal for Each Sex.

Sex	ROI	Brain Area (Atlas)	% Atlas Covered	# Of Voxels
Female (FAD v FCN)	Right Hippocampus	Right Hippocampus	47%	331
	Left Hippocampus Left	Left Hippocampus	53%	524
Male (MAD v MCN)	Right Hippocampus	Right Hippocampus	76%	527
		Left Hippocampus	20%	155
	Left Hippocampus	Left Hippocampus	68%	514
		Right Hippocampus	31%	216

In AD, males showed significantly stronger connectivity between the right and left hippocampus. This difference is shown visually by comparing boxes A and D in **Figure 3.3.1** and **Figure 3.3.2**.

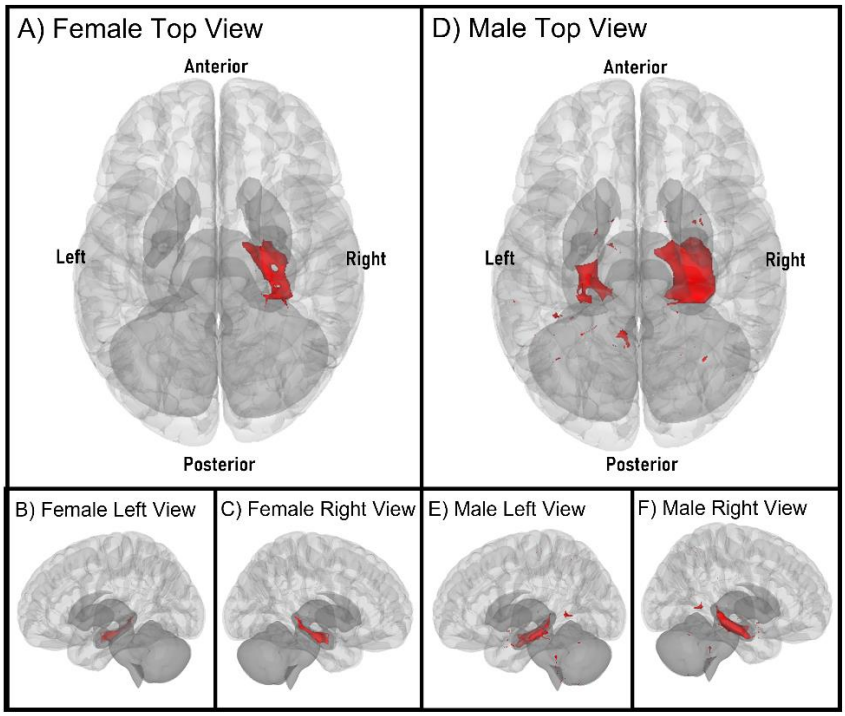

Figure 3.3.1 Sex-Specific Pathological Features with Right Hippocampus as ROI. Highlighted display the statistically significant cortical regions between Alzheimer's Disease (AD) and cognitively normal (CN) (p<0.001). A, B, and C display FAD v FCN. D, E, and F display MAD v MCN

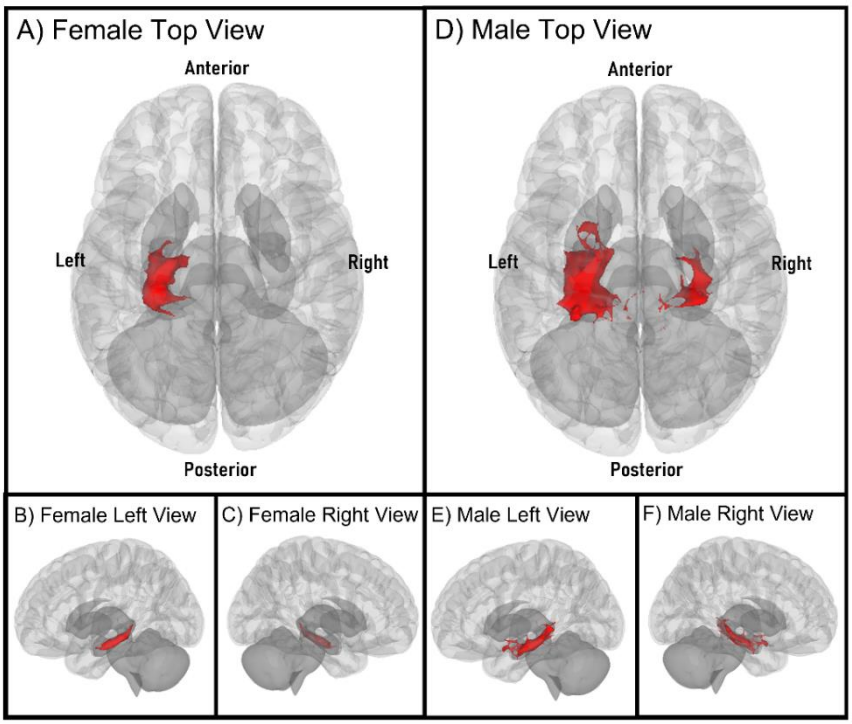

Figure 3.3.2 Sex-Specific Pathological Features with Left Hippocampus as ROI. Highlighted display the statistically significant cortical regions between Alzheimer's Disease (AD) and

cognitively normal (CN) (p<0.001). A, B, and C display FAD v FCN. D, E, and F display MAD v MCN

Discussion

This study supports the hypothesis that there are sex differences in cortical pathophysiological biomarkers in AD. Specifically, it expands the current understanding of hippocampal communication, demonstrating that there is a sex difference in interhemispheric functional connectivity between the left and right hippocampus.

Previous comprehensive studies have demonstrated disconnection deficits of interhemispheric cortical pathways are associated with AD [158-161]. In particular, these studies have found that functional interhemispheric hippocampal connectivity is decreased in Alzheimer's compared to controls [162, 163]. The communication of the left and right hippocampus is facilitated by the dorsal hippocampal commissure (DHC). The DHC is a white matter tract crossing the midline beneath the corpus callosum, providing interhemispheric connection between temporal lobe regions [164]. This tract has been suggested to play a key role in memory, particularly recognition memory [165]. However, the differences found in previous studies have not, to our knowledge, been extended to sex-specific differences. This finding may in part be a contributory factor in the observed worse neuropsychological task performance seen in females.

Unlike our previous study with MCI subjects [156], we did not observe sex differences in functional connectivity between the hippocampus and precuneus cortex or the brain stem. The precuneus cortex, specifically, has been shown to be related to the prodromal stages of AD [145, 166]. The precuneus cortex is known to exhibit early brain atrophy and is considered a vulnerable region for the transitional stage between MCI and dementia [167]. Therefore, it may be that the hippocampus-precuneus cortex functional connectivity is only a biomarker of MCI. This finding

may provide rational for the use of the precuneus cortex as good target for tailored sex-specific intervention, such as non-invasive brain stimulation (NIBS) [168, 169], to decrease the progression of MCI to AD.

Limitations and Future Work are related to this study's number of subjects. While this research provides preliminary findings on sex differences in functional connectivity of the hippocampus in AD, the small sample size (n=64) is a limitation. Therefore, future work includes increasing sample size in a larger database, as well as expanding functional connectivity from other regions of interest for AD, in addition to the hippocampus. Furthermore, studies such as these could be enhanced by combining aforementioned risk factors such as cognitive reserve or genetic differences to explore potential connections.

Chapter 4: Conclusion

The conclusions to this thesis are as followed:

- The results of the early data on the pilot clinical trial support the hypotheses that both facilitating ipsilesional primary motor cortex or inhibiting contralesional dorsal premotor area with HD-tDCS improves the excitability of the damaged cortico-spinal tract and/or reduces hyperexcitability of the cortico-reticulospinal tract to improve motor function of the upper extremity. The findings of this proof-of-concept study motivate further exploration of this topic, specifically, for more impaired individuals with high spasticity. These results may provide a foundation for continued clinical trial application of HD-tDCS for stroke rehabilitation. Additionally, the work on cortical sensory impairment and reorganization provide evidence for an EEG based sensory biomarker for the level of sensory and motor impairment post stroke, which has clinical importance for more impaired individuals.
- The studies of sex-specific functional connectivity differences of the hippocampus in MCI and AD support that there are cortical pathophysiological differences between sexes. Understanding these sex differences may aid in the development of sex-specific precision medicine to manipulate hippocampal-precuneus cortex and hippocampal-brainstem connectivity to decrease the progression of MCI to AD or in interhemispheric hippocampus connectivity as a treatment for AD.
- The future work of this research is exploring biomarkers of the relationship between stroke and AD. This is due to these conditions being intimately related, as AD can cause stroke and vice versa, as well as stroke can worsen the symptoms of existing dementia.

Funding

For the research on Alzheimer's Disease the work is supported by a seed grant from the Vice President for Research and Partnerships of the University of Oklahoma and the Data Institute for Societal Challenges. This work was also supported by the NIH/NICHD R01HD109157, NSF 2236459, American Heart Association (no. 932980 and 966924), Oklahoma Shared Clinical and Translational Resources (U54GM104938) with an Institutional Development Award from National Institute of General Medical Sciences, NIA-supported Geroscience Training Program in Oklahoma (T32AG052363), Oklahoma Nathan Shock Center (P30AG050911), and Cellular and Molecular GeroScience CoBRE (P20GM125528)

References

1. *2021 Profile of Older Americans*, U.S.D.o.H.a.H.S.A.f.C. Living, Editor. 2022.
2. Mather, M., L.A. Jacobsen, and K.M. Pollard, *Aging in the united states*. 2015: Population Reference Bureau.
3. Suzman, R. and J. Beard, *Global health and aging: preface. National Institute on Aging website*. 2015.
4. *Public Health and Aging: Trend in Aging - United States and Worldwide* Center for Disease Control 2003; Available from: https://www.cdc.gov/mmwr/preview/mmwrhtml/mm5206a2.htm#:~:text=The%20growing%20number%20of%20older%20adults%20increases%20demands,of%20life%2C%20and%20increased%20health-%20and%20long-term--care%20costs.
5. *Health and Economic Costs of Chronic Diseases*. 2020; Available from: https://www.cdc.gov/chronicdisease/about/costs/index.htm.
6. Lancet, T., *Moving toward precision medicine*. 2011, Elsevier. p. 1678.
7. Kosorok, M.R. and E.B. Laber, *Precision medicine.* Annual review of statistics and its application, 2019. **6**: p. 263-286.
8. Tan, L., et al., *Toward precision medicine in neurological diseases.* Ann Transl Med, 2016. **4**(6): p. 104.
9. *What is a Stroke*. 2022 March 21 2022]; Available from: https://www.nhlbi.nih.gov/health/stroke.
10. *Types of Strokes* 2023 March 21 2022]; Available from: https://www.hopkinsmedicine.org/health/conditions-and-diseases/stroke/types-of-stroke#:~:text=Strokes%20can%20be%20classified%20into%202%20main%20categories%3A,bleeding.%20About%2013%25%20of%20all%20strokes%20are%20hemorrhagic.
11. Virani, S.S., et al., *Heart disease and stroke statistics—2020 update: a report from the American Heart Association.* Circulation, 2020. **141**(9): p. e139-e596.

12. Langhorne, P., J. Bernhardt, and G. Kwakkel, *Stroke rehabilitation.* The Lancet, 2011. **377**(9778): p. 1693-1702.
13. Nudo, R.J., et al., *Neural substrates for the effects of rehabilitative training on motor recovery after ischemic infarct.* Science, 1996. **272**(5269): p. 1791-1794.
14. Belagaje, S.R., *Stroke rehabilitation.* CONTINUUM: Lifelong Learning in Neurology, 2017. **23**(1): p. 238-253.
15. Li, S., *Post-stroke spasticity, motor recovery and disordered motor control/S.* Li Front Neurol, 2017. **8**: p. 120.
16. Parker, V.M., D.T. Wade, and R. Langton Hewer, *Loss of arm function after stroke: measurement, frequency, and recovery.* Int Rehabil Med, 1986. **8**(2): p. 69-73.
17. Li, S., *Spasticity, Motor Recovery, and Neural Plasticity after Stroke.* Front Neurol, 2017. **8**: p. 120.
18. Li, S., et al., *A Unifying Pathophysiological Account for Post-stroke Spasticity and Disordered Motor Control.* Front Neurol, 2019. **10**: p. 468.
19. McPherson, J.G., et al., *Progressive recruitment of contralesional cortico-reticulospinal pathways drives motor impairment post stroke.* J Physiol, 2018. **596**(7): p. 1211-1225.
20. Tian, R., J.P.A. Dewald, and Y. Yang, *Assessing the Usage of Indirect Motor Pathways Following a Hemiparetic Stroke.* IEEE Trans Neural Syst Rehabil Eng, 2021. **29**: p. 1568-1572.
21. Jang, S.H. and S.J. Lee, *Corticoreticular tract in the human brain: a mini review.* Frontiers in Neurology, 2019. **10**: p. 1188.
22. Schwerin, S.C., J. Yao, and J.P. Dewald, *Using paired pulse TMS to facilitate contralateral and ipsilateral MEPs in upper extremity muscles of chronic hemiparetic stroke patients.* Journal of Neuroscience Methods, 2011. **195**(2): p. 151-160.
23. Bestmann, S., et al., *The role of contralesional dorsal premotor cortex after stroke as studied with concurrent TMS-fMRI.* Journal of Neuroscience, 2010. **30**(36): p. 11926-11937.
24. Orrù, G., et al., *Motor stroke recovery after tDCS: a systematic review.* Reviews in the Neurosciences, 2020. **31**(2): p. 201-218.
25. Mackenbach, C., R. Tian, and Y. Yang. *Effects of electrode configurations and injected current intensity on the electrical field of transcranial direct current stimulation: A simulation study*. in *2020 42nd Annual International Conference of the IEEE Engineering in Medicine & Biology Society (EMBC)*. 2020. IEEE.
26. Gladstone, D.J., C.J. Danells, and S.E. Black, *The Fugl-Meyer Assessment of Motor Recovery after Stroke: A Critical Review of Its Measurement Properties.* Neurorehabilitation and Neural Repair, 2002. **16**(3): p. 232-240.
27. Schwerin, S., et al., *Ipsilateral versus contralateral cortical motor projections to a shoulder adductor in chronic hemiparetic stroke: implications for the expression of arm synergies.* Exp Brain Res, 2008. **185**(3): p. 509-19.
28. Oliveri, M., et al., *Paired transcranial magnetic stimulation protocols reveal a pattern of inhibition and facilitation in the human parietal cortex.* The Journal of physiology, 2000. **529**(2): p. 461-468.
29. Tscherpel, C., et al., *The differential roles of contralesional frontoparietal areas in cortical reorganization after stroke.* Brain stimulation, 2020. **13**(3): p. 614-624.
30. Tscherpel, C., et al., *Age affects the contribution of ipsilateral brain regions to movement kinematics.* Human brain mapping, 2020. **41**(3): p. 640-655.

31. Stephan, M.A., et al., *Melodic priming of motor sequence performance: The role of the dorsal premotor cortex.* Frontiers in Neuroscience, 2016. **10**: p. 210.
32. Stinear CM, B.W., Ackerley SJ, Smith MC, Borges VM, Barber PA. , *PREP2: A biomarker-based algorithm for predicting upper limb function after stroke.* Annals of Clinical Translational Neurology, 2017. **4**(11): p. 811-820.
33. Gbadeyan, O., et al., *Safety, Tolerability, Blinding Efficacy and Behavioural Effects of a Novel MRI-Compatible, High-Definition tDCS Set-Up.* Brain Stimul, 2016. **9**(4): p. 545-52.
34. Godinho, M.M., et al., *Safety of transcranial direct current stimulation: Evidence based update 2016.* Brain Stimul, 2017. **10**(5): p. 983-985.
35. Huang, Y., et al., *Realistic volumetric-approach to simulate transcranial electric stimulation—ROAST—a fully automated open-source pipeline.* Journal of neural engineering, 2019. **16**(5): p. 056006.
36. Li, P., et al., *Altered excitability of motor neuron pathways after stroke: more than upper motor neuron impairments.* Stroke and Vascular Neurology, 2022. **7**(6): p. 518-526.
37. Escudero, J.V., et al., *Prognostic Value of Motor Evoked Potential Obtained by Transcranial Magnetic Brain Stimulation in Motor Function Recovery in Patients With Acute Ischemic Stroke.* Stroke, 1998. **29**(9): p. 1854-1859.
38. Karatzetzou, S., et al., *Transcranial magnetic stimulation implementation on stroke prognosis.* Neurological Sciences, 2022. **43**(2): p. 873-888.
39. Hiragami, S., Y. Inoue, and K. Harada, *Minimal clinically important difference for the Fugl-Meyer assessment of the upper extremity in convalescent stroke patients with moderate to severe hemiparesis.* Journal of physical therapy science, 2019. **31**(11): p. 917-921.
40. Kim, H., et al., *Task-Related Hemodynamic Changes Induced by High-Definition Transcranial Direct Current Stimulation in Chronic Stroke Patients: An Uncontrolled Pilot fNIRS Study.* Brain Sciences, 2022. **12**(4): p. 453.
41. Bao, S.C., et al., *Cortico-Muscular Coherence Modulated by High-Definition Transcranial Direct Current Stimulation in People With Chronic Stroke.* IEEE Trans Neural Syst Rehabil Eng, 2019. **27**(2): p. 304-313.
42. Priori, A., et al., *Polarization of the human motor cortex through the scalp.* Neuroreport, 1998. **9**(10): p. 2257-2260.
43. Samani, M.M., et al., *Titrating the neuroplastic effects of cathodal transcranial direct current stimulation (tDCS) over the primary motor cortex.* Cortex, 2019. **119**: p. 350-361.
44. Pillen, S., et al., *No robust online effects of transcranial direct current stimulation on corticospinal excitability.* Brain Stimulation, 2022. **15**(5): p. 1254-1268.
45. Horvath, J.C., J.D. Forte, and O. Carter, *Evidence that transcranial direct current stimulation (tDCS) generates little-to-no reliable neurophysiologic effect beyond MEP amplitude modulation in healthy human subjects: A systematic review.* Neuropsychologia, 2015. **66**: p. 213-236.
46. McPherson, J.G., et al., *Neuromodulatory inputs to motoneurons contribute to the loss of independent joint control in chronic moderate to severe hemiparetic stroke.* Frontiers in neurology, 2018. **9**: p. 470.
47. J.O. Dolly, K.R.A., *The structure and mode of action of different botulinum toxins.* European Journal of Neurology 2006 **13**(s4): p. 1-9.

48. Lisa C. Shaw, C.I.M.P., Frederike M.J. van Wijck, Phil Shackley, Nick Steen, Michael P. Barnes, Gary A. Ford, Laura A. Graham and Helen Rodgers, *Botulinum Toxin for the Upper Limb After Stroke (BoTULS) Trial.* Stroke, 2011. **42**: p. 1371-1379.
49. Santamato, A., et al., *Efficacy and safety of higher doses of botulinum toxin type A NT 201 free from complexing proteins in the upper and lower limb spasticity after stroke.* Journal of Neural Transmission, 2013. **120**(3): p. 469-476.
50. Teasell, R., et al., *Evidence to Practice: Botulinum Toxin in the Treatment of Spasticity Post Stroke.* Topics in Stroke Rehabilitation, 2012. **19**(2): p. 115-121.
51. Cramer, S.C., *Repairing the human brain after stroke: I. Mechanisms of spontaneous recovery.* Annals of neurology, 2008. **63**(3): p. 272-287.
52. Dromerick, A.W., et al., *Critical Period After Stroke Study (CPASS): A phase II clinical trial testing an optimal time for motor recovery after stroke in humans.* Proc Natl Acad Sci U S A, 2021. **118**(39).
53. Grefkes, C. and G.R. Fink, *Recovery from stroke: current concepts and future perspectives.* Neurological research and practice, 2020. **2**(1): p. 1-10.
54. Gill, J., P.P. Shah-Basak, and R. Hamilton, *It's the Thought That Counts: Examining the Task-dependent Effects of Transcranial Direct Current Stimulation on Executive Function.* Brain Stimulation, 2015. **8**(2): p. 253-259.
55. Solomons, C.D. and V. Shanmugasundaram, *A review of transcranial electrical stimulation methods in stroke rehabilitation.* Neurology India, 2019. **67**(2): p. 417.
56. Ellis, M.D., et al., *Progressive Abduction Loading Therapy with Horizontal-Plane Viscous Resistance Targeting Weakness and Flexion Synergy to Treat Upper Limb Function in Chronic Hemiparetic Stroke: A Randomized Clinical Trial.* Front Neurol, 2018. **9**(9): p. 71.
57. Clinic, C. *Median Nerve*. 2021 10/11/2022]; Available from: https://my.clevelandclinic.org/health/body/21889-median-nerve.
58. Liu, S., Dan J. Kopacz, and Randall L. Carpenter, *Quantitative Assessment of Differential Sensory Nerve Block after Lidocaine Spinal Anesthesia* Anesthesiology, 1995. **82**(1): p. 60-63.
59. Morita, G., et al., *Estimation of the conduction velocity distribution of human sensory nerve fibers.* Journal of Electromyography and Kinesiology, 2002. **12**(1): p. 37-43.
60. Alsuradi, H., W. Park, and M. Eid, *EEG-Based Neurohaptics Research: A Literature Review.* IEEE Access, 2020. **8**: p. 49313-49328.
61. Deschrijver, E., Wiersema, J. R., & Brass, M., *The interaction between felt touch and tactile consequences of observed actions: an action-based somatosensory congruency paradigm.* Social Cognitive and Affective Neuroscience, 2016. **11**(7): p. 1162-1172.
62. Filatova, O.G., et al., *Dynamic Information Flow Based on EEG and Diffusion MRI in Stroke: A Proof-of-Principle Study.* Front Neural Circuits, 2018. **12**: p. 79.
63. Inanc G., Ö., M., and Öniz, A., *Sensory brain responses and lateralization in nonpainful tactile stimuli during sleep.* Neurol Sci Neurophysiol, 2021. **38**: p. 12-9.
64. Arnaud Delorme, S.M., *EEGLAB: an open source toolbox for analysis of single-trial EGG dynamics including independent component analysis.* Journal of Neuroscience Methods, 2004. **134**: p. 9-21.
65. Pascual-Marqui, R.D., *Standardized low-resolution brain electromagnetic tomography (sLORETA): technical details.* Methods Find Exp Clin Pharmacol, 2002. **24**(Suppl D): p. 5-12.

66. Yao, J., Dewald, J.P., *Evaluation of different cortical source localization methods using simulated and experimental EEG data.* NeuroImage, 2005. **25**: p. 369-382.
67. Galin, D. and R.R. Ellis, *Asymmetry in evoked potentials as an index of lateralized cognitive processes: Relation to EEG alpha asymmetry.* Neuropsychologia, 1975. **13**(1): p. 45-50.
68. Tian, R., J.P. Dewald, and Y. Yang, *Assessing the usage of indirect motor pathways following a hemiparetic stroke.* IEEE Transactions on Neural Systems and Rehabilitation Engineering, 2021. **29**: p. 1568-1572.
69. Filatova OG, Y.Y., Dewald JPA, Tian R, Maceira-Elvira P, Takeda Y, Kwakkel G, Yamashita O and van der Helm FCT, *Dynamic Information Flow Based on EEG and Diffusion MRI in Stroke: A Proof-of-Principle Study.* Front. Neural Circuits, 2018. **12:79**.
70. Oniz, A., Inanc, G., Guducu, C., and Ozgoren, M., *Brain responsiveness to non-painful tactile stimuli prior and during sleep.* Sleep Biol. Rhythms, 2016. **14**: p. 87-96.
71. Zhang, D., Xu, F., Xu, H., Shull, P. B., and Zhu, X., *Quantifying different tactile sensations evoked by cutaneous electrical stimulation using electroencephalography features.* Int. J. Neural Syst., 2016. **26:1650006**.
72. Grefkes, C. and G.R. Fink, *Reorganization of cerebral networks after stroke: new insights from neuroimaging with connectivity approaches.* Brain, 2011. **134**(5): p. 1264-1276.
73. Wilkins, K.B., et al., *Neural Plasticity in Moderate to Severe Chronic Stroke Following a Device-Assisted Task-Specific Arm/Hand Intervention.* Front Neurol, 2017. **8**: p. 284.
74. Tian, R., Dewald, J. P., & Yang, Y. , *Assessing the usage of indirect motor pathways following a hemiparetic stroke.* IEEE Transactions on Neural Systems and Rehabilitation Engineering, 2021. **29**.
75. Borich, M.R., C. Mang, and L.A. Boyd, *Both projection and commissural pathways are disrupted in individuals with chronic stroke: investigating microstructural white matter correlates of motor recovery.* BMC Neuroscience, 2012. **13**(1): p. 107.
76. Fabri, M., et al., *Contribution of posterior corpus callosum to the interhemispheric transfer of tactile information.* Cognitive Brain Research, 2005. **24**(1): p. 73-80.
77. Fabri, M., et al., *Posterior Corpus Callosum and Interhemispheric Transfer of Somatosensory Information: An fMRI and Neuropsychological Study of a Partially Callosotomized Patient.* Journal of Cognitive Neuroscience, 2001. **13**(8): p. 1071-1079.
78. Arya, K.N., *Underlying neural mechanisms of mirror therapy: Implications for motor rehabilitation in stroke.* Neurology India, 2016. **64**(1): p. 38-44.
79. Campfens, S.F., et al., *Stretch Evoked Potentials in Healthy Subjects and After Stroke: A Potential Measure for Proprioceptive Sensorimotor Function.* IEEE Trans Neural Syst Rehabil Eng, 2015. **23**(4): p. 643-54.
80. Yamada, T., et al., *Short- and Long-Latency Median Somatosensory Evoked Potentials: Findings in Patients With Localized Neurological Lesions.* Archives of Neurology, 1983. **40**(4): p. 215-220.
81. Meyke R., B.J.R., Renzenbrinkb G.J., Geurtsc A.C.H., IJzermand M.J., *Altered cortical somatosensory processing in chronic stroke: A relationship with post-stroke shoulder pain.* NeuroRehabilitation, 2011. **28**: p. 331-344.
82. Keren, O., et al., *Upper limb somatosensory evoked potentials as a predictor of rehabilitation progress in dominant hemisphere stroke patients.* Stroke, 1993. **24**(12): p. 1789-1793.

83. Bolognini, N., C. Russo, and D. Edwards, *The sensory side of post-stroke motor rehabilitation.* Restorative Neurology and Neuroscience, 2016. **34**: p. 571-586.
84. Reding, M.J. and E. Potes, *Rehabilitation outcome following initial unilateral hemispheric stroke. Life table analysis approach.* Stroke, 1988. **19**(11): p. 1354-8.
85. Marconi, B., et al., *Long-term effects on cortical excitability and motor recovery induced by repeated muscle vibration in chronic stroke patients.* Neurorehabil Neural Repair, 2011. **25**(1): p. 48-60.
86. Toscano, M., et al., *Motor Recovery After Stroke: From a Vespa Scooter Ride Over the Roman Sampietrini to Focal Muscle Vibration (fMV) Treatment. A 99mTc-HMPAO SPECT and Neurophysiological Case Study.* Frontiers in Neurology, 2020. **11**.
87. Seim, C.E., S.L. Wolf, and T.E. Starner, *Wearable vibrotactile stimulation for upper extremity rehabilitation in chronic stroke: clinical feasibility trial using the VTS Glove.* Journal of NeuroEngineering and Rehabilitation, 2021. **18**(1): p. 14.
88. Karime, A., et al. *E-Glove: An electronic glove with vibro-tactile feedback for wrist rehabilitation of post-stroke patients*. in *2011 IEEE International Conference on Multimedia and Expo*. 2011.
89. Kim, H., H. Kim, and W.-S. Shin, *Effects of Vibrotactile Biofeedback Providing Real-Time Pressure Information on Static Balance Ability and Weight Distribution Symmetry Index in Patients with Chronic Stroke.* Brain Sciences, 2022. **12**(3): p. 358.
90. Yeh, I.L., et al., *Effects of a robot-aided somatosensory training on proprioception and motor function in stroke survivors.* Journal of NeuroEngineering and Rehabilitation, 2021. **18**(1): p. 77.
91. *What is Alzheimer's Disease*. 2021 March 22 2023]; Available from: https://www.nia.nih.gov/health/what-alzheimers-disease.
92. *What is Dementia? Symptoms, Types, and Diagnosis* 2022 March 22 2023]; Available from: https://www.nia.nih.gov/health/what-is-dementia.
93. Health, N.I.o. *Alzheimer's Disease*. 2021 1/30/2023]; Available from: https://www.nih.gov/research-training/accelerating-medicines-partnership-amp/alzheimers-disease#:~:text=It%20is%20the%20most%20common,to%2013.8%20million%20by%202050.
94. *2022 Alzheimer's disease facts and figures.* Alzheimers Dement, 2022. **18**(4): p. 700-789.
95. Kelley, A.S., et al., *The burden of health care costs for patients with dementia in the last 5 years of life.* Ann Intern Med, 2015. **163**(10): p. 729-36.
96. Scheltens, P., et al., *Alzheimer's disease.* The Lancet, 2016. **388**(10043): p. 505-517.
97. A. Armstrong, R., *Risk factors for Alzheimer's disease.* Folia Neuropathologica, 2019. **57**(2): p. 87-105.
98. Reitz, C., *Toward precision medicine in Alzheimer's disease.* Ann Transl Med, 2016. **4**(6): p. 107.
99. Berkowitz, C.L., et al. *Precision medicine for Alzheimer's disease prevention*. in *Healthcare*. 2018. MDPI.
100. van den Heuvel, M.P. and O. Sporns, *Network hubs in the human brain.* Trends in Cognitive Sciences, 2013. **17**(12): p. 683-696.
101. Stam, C.J., *Modern network science of neurological disorders.* Nat Rev Neurosci, 2014. **15**(10): p. 683-95.

102. Yu, M., et al., *Selective impairment of hippocampus and posterior hub areas in Alzheimer's disease: an MEG-based multiplex network study.* Brain, 2017. **140**(5): p. 1466-1485.
103. de Haan, W., et al., *Disruption of functional brain networks in Alzheimer's disease: what can we learn from graph spectral analysis of resting-state magnetoencephalography?* Brain Connect, 2012. **2**(2): p. 45-55.
104. Snyder, H.M., et al., *Sex biology contributions to vulnerability to Alzheimer's disease: A think tank convened by the Women's Alzheimer's Research Initiative.* Alzheimer's & Dementia, 2016. **12**(11): p. 1186-1196.
105. Guerreiro, R. and J. Bras, *The age factor in Alzheimer's disease.* Genome medicine, 2015. **7**(1): p. 1-3.
106. Davis, E.J., et al., *A second X chromosome contributes to resilience in a mouse model of Alzheimer's disease.* Sci Transl Med, 2020. **12**(558).
107. Andrew, M.K. and M.C. Tierney, *The puzzle of sex, gender and Alzheimer's disease: Why are women more often affected than men?* Women's Health, 2018. **14**: p. 1745506518817995.
108. Mielke, M.M., *Sex and Gender Differences in Alzheimer's Disease Dementia.* Psychiatr Times, 2018. **35**(11): p. 14-17.
109. Mielke, M.M., et al., *Consideration of sex and gender in Alzheimer's disease and related disorders from a global perspective.* Alzheimer's & Dementia, 2022.
110. Pearce, E.E., et al., *Telomere length and epigenetic clocks as markers of cellular aging: a comparative study.* Geroscience, 2022. **44**(3): p. 1861-1869.
111. Sienski, G., et al., *APOE4 disrupts intracellular lipid homeostasis in human iPSC-derived glia.* Sci Transl Med, 2021. **13**(583).
112. Association, A.s., *2016 Alzheimer's Disease Facts and Figures* Alzheimer's & Dementia, 2016. **12**(4): p. 459-509.
113. Sohn, D., et al., *Sex differences in cognitive decline in subjects with high likelihood of mild cognitive impairment due to Alzheimer's disease.* Scientific reports, 2018. **8**(1): p. 7490.
114. Henderson, V.W. and J.G. Buckwalter, *Cognitive deficits of men and women with Alzheimer's disease.* Neurology, 1994. **44**(1): p. 90-6.
115. Chapman, R.M., et al., *Women have farther to fall: gender differences between normal elderly and Alzheimer's disease in verbal memory engender better detection of Alzheimer's disease in women.* Journal of the International Neuropsychological Society, 2011. **17**(4): p. 654-662.
116. Gumus, M., et al., *Progression of neuropsychiatric symptoms in young-onset versus late-onset Alzheimer's disease.* Geroscience, 2021. **43**: p. 213-223.
117. Heise, V., et al., *Apolipoprotein E genotype, gender and age modulate connectivity of the hippocampus in healthy adults.* Neuroimage, 2014. **98**: p. 23-30.
118. Ferretti, M.T., et al., *Sex differences in Alzheimer disease - the gateway to precision medicine.* Nat Rev Neurol, 2018. **14**(8): p. 457-469.
119. Jiang, J., et al., *Glucose metabolism patterns: A potential index to characterize brain ageing and predict high conversion risk into cognitive impairment.* GeroScience, 2022. **44**(4): p. 2319-2336.

120. Burke, S.L., et al., *Sex differences in the development of mild cognitive impairment and probable Alzheimer's disease as predicted by hippocampal volume or white matter hyperintensities.* Journal of Women & Aging, 2019. **31**(2): p. 140-164.
121. Ardekani, B.A., A. Convit, and A.H. Bachman, *Analysis of the MIRIAD Data Shows Sex Differences in Hippocampal Atrophy Progression.* Journal of Alzheimer's Disease, 2016. **50**: p. 847-857.
122. Cavedo, E., et al., *Sex differences in functional and molecular neuroimaging biomarkers of Alzheimer's disease in cognitively normal older adults with subjective memory complaints.* Alzheimer's & Dementia, 2018. **14**(9): p. 1204-1215.
123. Rahman, A., et al., *Sex-driven modifiers of Alzheimer risk: a multimodality brain imaging study.* Neurology, 2020. **95**(2): p. e166-e178.
124. Petersen, R.C., *Mild cognitive impairment as a diagnostic entity.* Journal of internal medicine, 2004. **256**(3): p. 183-194.
125. Salmon, D.P., *Neuropsychological features of mild cognitive impairment and preclinical Alzheimer's disease.* Behavioral neurobiology of aging, 2012: p. 187-212.
126. Gauthier, S., et al., *Mild cognitive impairment.* The lancet, 2006. **367**(9518): p. 1262-1270.
127. Davatzikos, C., et al., *Prediction of MCI to AD conversion, via MRI, CSF biomarkers, and pattern classification.* Neurobiology of aging, 2011. **32**(12): p. 2322. e19-2322. e27.
128. McGrattan, A.M., et al., *Risk of conversion from mild cognitive impairment to dementia in low-and middle-income countries: a systematic review and meta-analysis.* Alzheimer's & Dementia: Translational Research & Clinical Interventions, 2022. **8**(1): p. e12267.
129. López, M.E., et al., *A multivariate model of time to conversion from mild cognitive impairment to Alzheimer's disease.* Geroscience, 2020. **42**: p. 1715-1732.
130. Braak, H. and E. Braak, *Staging of Alzheimer's disease-related neurofibrillary changes.* Neurobiology of aging, 1995. **16**(3): p. 271-278.
131. Weiner, M.W., *Alzheimer's Disease Neuroimaging Initiative.* 2016.
132. S. Whitfield-Gabriel, A.N.-C., *Conn: a functional connectivity toolbox for correlated and anticorrelated brain networks.* Brain Connect, 2012. **2**(3): p. 125-141.
133. Jenkinson, M., et al., *Fsl.* Neuroimage, 2012. **62**(2): p. 782-790.
134. Woolrich, M.W., et al., *Bayesian analysis of neuroimaging data in FSL.* Neuroimage, 2009. **45**(1 Suppl): p. S173-86.
135. Smith, S.M., et al., *Advances in functional and structural MR image analysis and implementation as FSL.* Neuroimage, 2004. **23**: p. S208-S219.
136. Tzourio-Mazoyer, N., et al., *Automated anatomical labeling of activations in SPM using a macroscopic anatomical parcellation of the MNI MRI single-subject brain.* Neuroimage, 2002. **15**(1): p. 273-289.
137. Nieto-Castanon, A., *Handbook of functional connectivity Magnetic Resonance Imaging methods in CONN*. 2020: Hilbert Press.
138. Whitfield-Gabrieli, S. and A. Nieto-Castanon, *Conn: a functional connectivity toolbox for correlated and anticorrelated brain networks.* Brain Connect, 2012. **2**(3): p. 125-41.
139. Worsley, K.J., et al., *A unified statistical approach for determining significant signals in images of cerebral activation.* Human brain mapping, 1996. **4**(1): p. 58-73.
140. Goel, A., *Parahippocampal gyrus.* 2015.

141. Weniger, G., K. Boucsein, and E. Irle, *Impaired associative memory in temporal lobe epilepsy subjects after lesions of hippocampus, parahippocampal gyrus, and amygdala.* Hippocampus, 2004. **14**(6): p. 785-796.
142. Wang, Z., et al., *Baseline and longitudinal patterns of hippocampal connectivity in mild cognitive impairment: Evidence from resting state fMRI.* Journal of the Neurological Sciences, 2011. **309**(1): p. 79-85.
143. Ortner, M., et al., *Progressively Disrupted Intrinsic Functional Connectivity of Basolateral Amygdala in Very Early Alzheimer's Disease.* Frontiers in Neurology, 2016. **7**.
144. Cavanna, A.E. and M.R. Trimble, *The precuneus: a review of its functional anatomy and behavioural correlates.* Brain, 2006. **129**(3): p. 564-583.
145. Rami, L., et al., *Distinct Functional Activity of the Precuneus and Posterior Cingulate Cortex During Encoding in the Preclinical Stage of Alzheimer's Disease.* Journal of Alzheimer's Disease, 2012. **31**: p. 517-526.
146. Yokoi, T., et al., *Involvement of the Precuneus/Posterior Cingulate Cortex Is Significant for the Development of Alzheimer's Disease: A PET (THK5351, PiB) and Resting fMRI Study.* Frontiers in Aging Neuroscience, 2018. **10**.
147. Kim, J., Y.-H. Kim, and J.-H. Lee, *Hippocampus–precuneus functional connectivity as an early sign of Alzheimer's disease: A preliminary study using structural and functional magnetic resonance imaging data.* Brain Research, 2013. **1495**: p. 18-29.
148. Serra, L., et al., *In vivo mapping of brainstem nuclei functional connectivity disruption in Alzheimer's disease.* Neurobiology of Aging, 2018. **72**: p. 72-82.
149. Jacobs, H.I.L., et al., *Relevance of parahippocampal-locus coeruleus connectivity to memory in early dementia.* Neurobiology of Aging, 2015. **36**(2): p. 618-626.
150. Osone, A., et al., *Impact of cognitive reserve on the progression of mild cognitive impairment to A lzheimer's disease in J apan.* Geriatrics & gerontology international, 2015. **15**(4): p. 428-434.
151. Giacomucci, G., et al., *Gender differences in cognitive reserve: Implication for subjective cognitive decline in women.* Neurological Sciences, 2022.
152. Kim, S., et al., *Gender differences in risk factors for transition from mild cognitive impairment to Alzheimer's disease: A CREDOS study.* Comprehensive Psychiatry, 2015. **62**: p. 114-122.
153. Hardcastle, C., et al., *Proximal improvement and higher-order resting state network change after multidomain cognitive training intervention in healthy older adults.* Geroscience, 2022. **44**(2): p. 1011-1027.
154. Yang, Y., E. Sidorov, and J.P. Dewald, *Targeted tDCS reduces the expression of the upper limb flexion synergy in chronic hemiparetic stroke.* Archives of Physical Medicine and Rehabilitation, 2021. **102**(10): p. e10.
155. Vecchio, F., et al., *Neuronavigated Magnetic Stimulation combined with cognitive training for Alzheimer's patients: an EEG graph study.* Geroscience, 2022: p. 1-14.
156. Williamson, J., et al., *Sex differences in brain functional connectivity of hippocampus in mild cognitive impairment.* Frontiers in Aging Neuroscience, 2022.
157. Weiner, M.W., *Alzheimer's Disease Neuroimaging Initiative.* 2016.
158. Rose, S.E., et al., *Loss of connectivity in Alzheimer's disease: an evaluation of white matter tract integrity with colour coded MR diffusion tensor imaging.* Journal of Neurology, Neurosurgery & Psychiatry, 2000. **69**(4): p. 528-530.

159. Delbeuck, X., M. Van der Linden, and F. Collette, *Alzheimer'disease as a disconnection syndrome?* Neuropsychology review, 2003. **13**: p. 79-92.
160. Morrison, J., et al., *The laminar and regional distribution of somatostatin and neuritic disconnection syndrome.* The Biological Substrates of Alzheimer's Disease, 1986: p. 115-131.
161. Reuter-Lorenz, P.A. and J.A. Mikels, *A split-brain model of Alzheimer's disease?: Behavioral evidence for comparable intra and interhemispheric decline.* Neuropsychologia, 2005. **43**(9): p. 1307-1317.
162. Manno, F.A., et al., *Early stage alterations in white matter and decreased functional interhemispheric hippocampal connectivity in the 3xTg mouse model of Alzheimer's disease.* Frontiers in aging neuroscience, 2019. **11**: p. 39.
163. Wang, Z., et al., *Interhemispheric functional and structural disconnection in Alzheimer's disease: a combined resting-state fMRI and DTI study.* PLoS One, 2015. **10**(5): p. e0126310.
164. Nasa, A., et al., *The human dorsal hippocampal commissure: Delineating connections across the midline using multi-modal neuroimaging in major depressive disorder.* Neuroimage: Reports, 2021. **1**(4): p. 100062.
165. Postans, M., et al., *Uncovering a Role for the Dorsal Hippocampal Commissure in Recognition Memory.* Cerebral Cortex, 2019. **30**(3): p. 1001-1015.
166. Franzmeier, N., et al., *Left frontal cortex connectivity underlies cognitive reserve in prodromal Alzheimer disease.* Neurology, 2017. **88**(11): p. 1054-1061.
167. Canter, R.G., J. Penney, and L.-H. Tsai, *The road to restoring neural circuits for the treatment of Alzheimer's disease.* Nature, 2016. **539**(7628): p. 187-196.
168. Casula, E.P., et al., *Regional precuneus cortical hyperexcitability in Alzheimer's disease patients.* Annals of Neurology, 2022.
169. Koch, G., et al., *Transcranial magnetic stimulation of the precuneus enhances memory and neural activity in prodromal Alzheimer's disease.* Neuroimage, 2018. **169**: p. 302-311.